The long time water absorption in the air-pore structure of concrete

Fagerlund, Göran

1993

LUND INSTITUTE OF TECHNOLOGY
Division of Building Materials

THE LONG TIME WATER ABSORPTION IN THE AIR-PORE STRUCTURE OF CONCRETE

Göran Fagerlund

Rapport TVBM-3051
Lund 1993

Preface

This report is produced within the BRITE/EURAM project BREU-CT92-0591 "The Residual Service Life of Concrete Structures".

Five partners are involved in the project:

1: British Cement Association. (The coordinator).
2: Instituto Eduardo Torroja, Spain.
3: Geocisa, Spain.
4: Swedish Cement and Concrete Research Institute.
5: Cementa AB, Sweden.
6: Div. Building Materials, Lund Inst. of Technol., Sweden.

Three deterioration mechanisms are treated in the project:

1: Corrosion of reinforcement.
2: Freeze-thaw effects.
3: Alkali silika reaction.

This report refers to Task 4 of the work, "Assessment of deterioration rates" ; sub-task 4.2 "Freeze-thaw".

Lund 25 March 1993.

Göran Fagerlund

1. Frost destruction. The critical water absorption. The service life

1.1 The critical size

A completely water saturated cement paste volume is severely damaged by frost if its size exceeds a certain critical volume /1/. The critical size depends on the lowest temperature used in the test and it depends on the salt concentrations outside and inside the volume /2/. It also is, to a certain extent, dependent of the freezing rate /3/. One can talk about a critical thickness of a thin slice of the paste or one can talk about a critical diameter of a spherical piece of the paste. Normally however, one uses the concept critical spacing factor L_{CR} which is the thickest water saturated cement paste shell surrounding an airpore. The shell is supposed to have an impermeable outer periphery. Thus, the critical spacing factor is the longest distance that water, that is expelled due to freezing, has to move before it reaches a recipient large enough to contain it. The spacing factor is a geometrical entity that is calculated on basis of the geometrical model shown in Fig 1.1. Thus, all airpores are supposed to have the same diameter ϕ defined by:

$$\phi = 6/\alpha_o \qquad (1.1)$$

Where α_o is the specific surface of the airpore system. This is defined by the total surface/volume ratio of all pores that are large enough not to become waterfilled too rapidly in practice. In the original derivation made by Powers /4/ all entrained and entrapped airpores were included in α_o. Then, the spacing factor L is /4/:

$$L = [3/\alpha_o] \cdot \{1,4[V_p/a_o+1]^{1/3}-1\} \qquad (1.2)$$

Where V_p is the volume fraction of cement paste (airpores excluded) and a_o is the total airpore volume.

The geometrical model behind Eq (1.2) is too simplified. A more general, statistical, spacing factor L´in which consideration can also be taken to the size distribution is derived in /5/. The following general equation is valid:

$$V_p\left\{1+0,5\cdot L'\cdot\alpha_o+0,5\cdot L'^2\cdot\alpha_o\cdot\frac{[u]_1}{[u]_2}+0,17\cdot L'^3\cdot\alpha_o\frac{[u]_o}{[u]_2}\right\} = C \qquad (1.3)$$

Where $[u]_i$ is the i:th statistical moment of the pore size distribution. This spacing factor implies that all points in the cement paste lies with a certain probability within the distance L´from the periphery of the nearest airpore. The probability that the whole cement paste volume is protected increases with

increasing value of the factor C. When C=1 the probability is 63%. When C=2,3 the probability is 90%. Thus, the spacing factor depends both on the pore size distribution, as does the Powers spacing factor according to Eq(1.2), but also on the probability that all parts of the cement paste shall be protected.

The critical Powers spacing factor L_{CR} is about 0,3 to 0,5 mm for freezing in pure water. Research is under way to obtain more accurate values for different water cement ratios, different salt solutions in the pore system etc.

1.2 The critical water absorption

The airpores will not stay air-filled but will take up water by a slow air dissolution-diffusion process that is described in section 3 below. This means that the residual spacing factor between pores that are still air-filled will increase with increasing time of water storage of the concrete. The relation between the residual spacing factor L_r and the degree of water-filling of the pore system can be calculated by Eq (1.2) when the residual specific surface α_r and the residual air volume a_r of pores that are not water-filled to such large extent that they cannot accomodate all water that is expelled from the surrounding cement paste shell, are known.

a_r is calculated by:

$$a_r = \int_{r_{min}}^{r_{max}} f(r) \cdot \frac{4\pi}{3} \cdot r^3 \cdot dr \qquad (1.4)$$

Where f(r) is the frequency function of pore radii. r_{min} is the radius of the smallest pore that cannot accomodate any expelled water. Such a pore might be a completely water-filled pore or a pore that is water-filled to such an extent that the residual air volume is smaller than 9% of the freezable water contained in the water-filled cement paste shell surrounding the pore. In these cases water has to move to another, coarser pore. r_{max} is the radius of the largest airpore. Eq (1.4) implies that a smaller pore is always water-filled before a larger pore. That this assumption is justified is shown by the analysis performed below in section 3.

The residual pore surface A_r is:

$$A_r = \int_{r_{min}}^{r_{max}} f(r) \cdot 4\pi \cdot r^2 \cdot dr \qquad (1.5)$$

Then, the residual specific surface of the portion of the air-pore system that is still air-filled, α_r is:

$$\alpha_r = A_r/a_r \qquad (1.6)$$

As a consequence of the gradual reduction in the residual air-pore volume and specific surface the residual spacing L_r between the airpores increase; see Eq (1.2) and (1.3).

$$L_r = [3/\alpha_r]\cdot\{1,4\cdot[V_p/a_r+1]^{1/3}-1\} \qquad (1.2a)$$

Hypothetical examples of the changes in α_r and a_r and are shown in Fig 1.2.

Frost destruction occurs when the degree of water-filling is so high that the critical spacing is exceeded ($L_r>L_{CR}$). Then, the residual airpore volume is $a_{r,CR}$. This means that there exists a critical degree of saturation $S_{a,CR}$ of the airpore system:

$$S_{a,CR} = 1- a_{r,CR}/a_o \qquad (0<S_{a,CR}<1) \qquad (1.7)$$

There also exists a critical degree of saturation S_{CR} of the entire material, capillary pores and gel pores included. They are always water-filled before the airpores start to take up water. Therefore, S_{CR} is defined:

$$S_{CR} = 1 - a_{r,CR}/P_{tot} \qquad (0<S_{CR}<1) \qquad (1.8)$$

Where P_{tot} is the total pore volume in the concrete. Thus, by knowing the total airpore volume and by measuring the weight gain of a concrete stored in water for a long time the gradual water absorption in the airpores can be followed. Then, by also investigating the pore size distribution one can find relations between the pore size and the rate of water absorption. Such analyses are made below in sections 3 and 4. Experimental results are presented in section 5.

The relaton between the two degrees of saturation is:

$$S_{a,CR} = 1 - \frac{P_{tot}(1-S_{CR})}{a_o} \qquad (1.9)$$

Two examples of the determination of the critical degree of saturation by freeze/thaw experiments are shown in Fig 1.3; /8/.

1.3 The service life

The water absorption process is time dependent:

$$S_a = S_a(t) \qquad (1.10)$$

The service life of a representative unit volume inside the concrete is ended when $S_a(t)$ exceeds the critical degree of saturation of the airpore system $S_{a,CR}$ which is supposed to be independent of time; at least for mature concrete.

The value of $S_{a,CR}$ can be calculated theoretically according to the principles desribed above, provided the value L_{CR} of the critical spacing factor is known. Another possibility is to determine the value of S_{CR} and $S_{a,CR}$ experimentally. Suitable methods are described in /6/.

The time function $S_a(t)$ is calculated theoretically according to the principles described below, or it is measured experimentally by successive weighings of specimens that are stored for a long time in water. The most rational method is to make an experimental water absorption test for a limited space of time (e.g. 2 weeks) and then extrapolate the water absorption function until the extrapolated value of $S_a(t)$ reaches the value of $S_{a,CR}$. The time when this happens is a sort of **potential service life**.

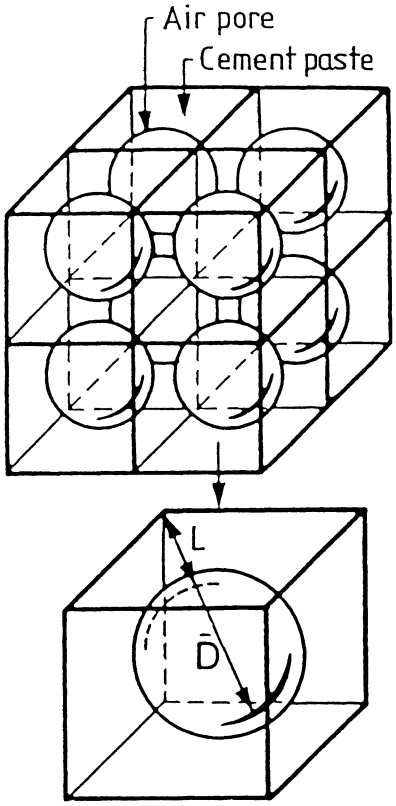

Fig 1.1: The geometrical airpore-cement paste model on which the Powers´spacing factor is based; /4/.

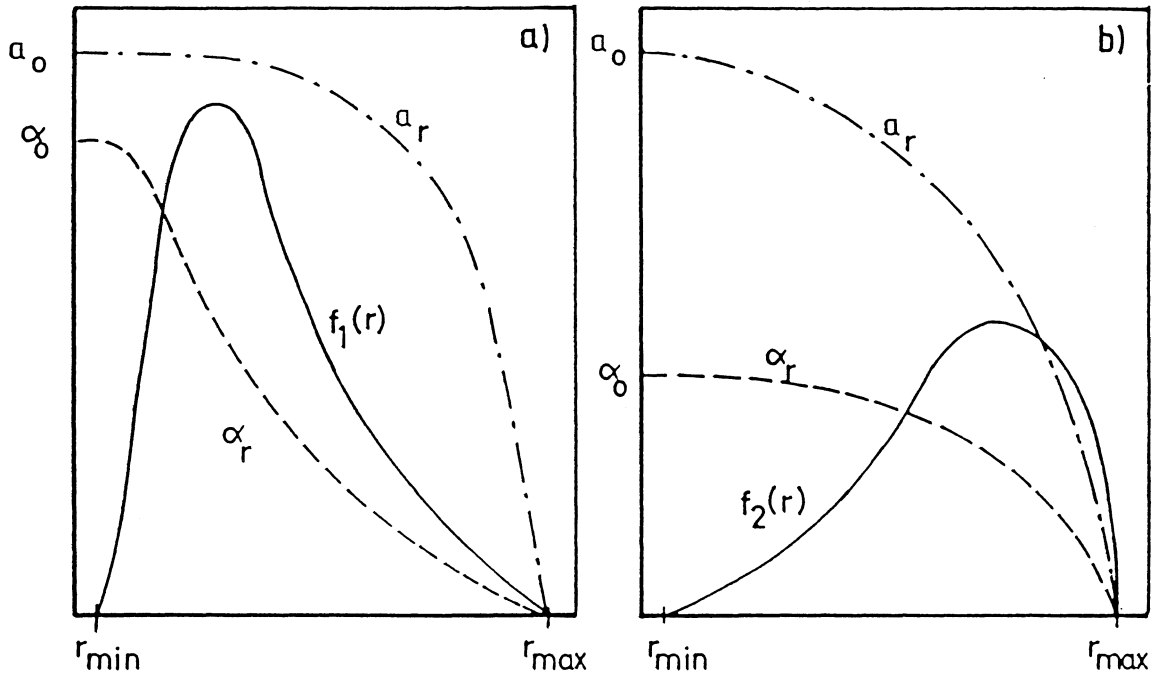

Fig 1.2: Hypothetical airpore distributions and the influence of a gradual water-filling on the residual volume, a_r, of pores that can still act as recipients for expelled water and the specific surface of such pores, α_r. (a) Fine-porous system. (b) Coarse-porous system.

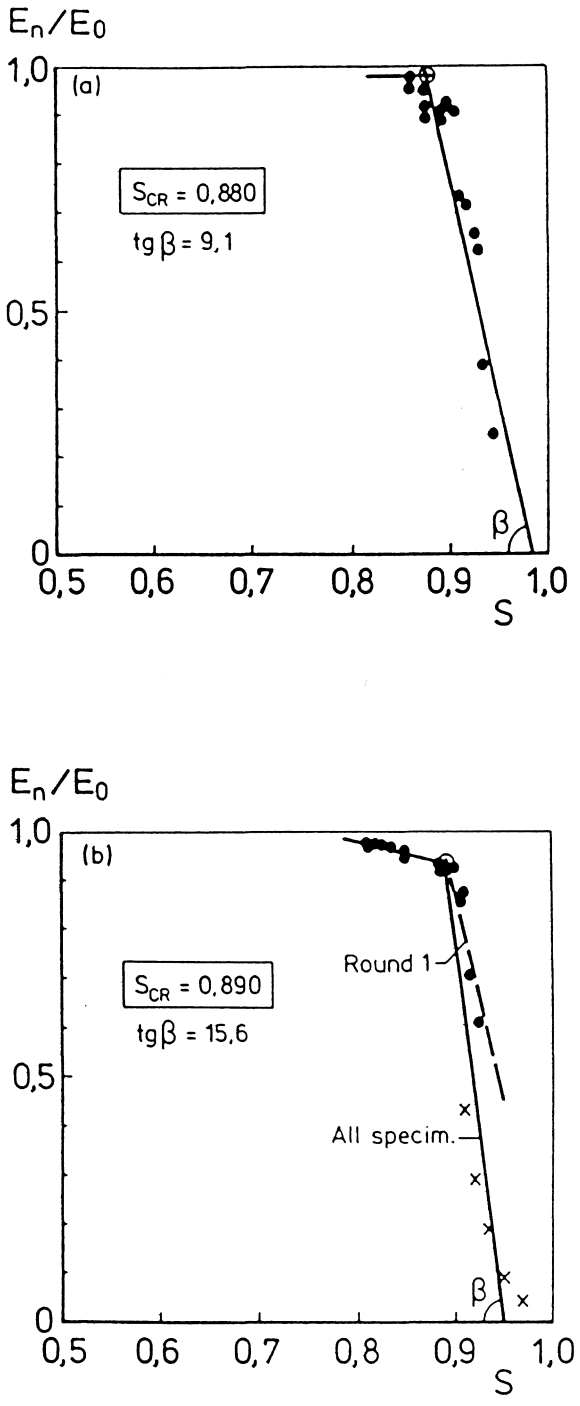

Fig 1.3: Example of determinations of the critical degree of saturation S_{CR}. Slag cement concretes with slag content 40 % and w/c-ratio 0,45; /8/.
(a) Air content 4,2 %. (b) Air content 5,4 %.

2. The capillary absorption process

When a piece of pre-dried concrete is placed in contact with a free water surface it immediately starts to take up water. A rather distinct water front penetrates the concrete; below the front, the gel and capillary pores are saturated, above the front, the water content is almost the same as it was initially. In reality, when the water front has advanced a bit, there will be a diffusion of water from the front which makes this a bit more diffuse. As long as only the first few centimeters are regarded and the concrete is not too dense the idea of a moving front is however acceptable.

The front moves according to this formula:

$$z = m \cdot \sqrt{t} \qquad (2.1)$$

where z is the distance from the water front to the free water surface and m is a material constant that can be called "the resistance to water penetration" [s/m^2]

The amount of water taken up W [kg/m^2] is:

$$W = k \cdot \sqrt{t} \qquad (2.2)$$

Where k is "the coefficient of capillarity" [$kg/(m^2 \cdot s^{1/2})$].

The relation between m and k is:

$$k = \frac{1000 \cdot P_{cap}}{\sqrt{m}} \qquad (2.3)$$

Where 1000 [kg/m^3] is the density of water and P_{cap} is "the active porosity" in the capillary process [m^3/m^3], i.e. the volume of pores that becomes water-filled already during the capillary process. Since normal airpores do not take part in this process, P_{cap} can be written:

$$P_{cap} = P_g + P_c - P_o \qquad (2.4)$$

Where P_g is the gel porosity, P_c is the capillary porosity and P_o is the porosity that was water-filled already when the capillary process started.

The water absorption rate q_c [$kg/(m^2 \cdot s)$] is:

$$q_c = \frac{k}{2 \cdot \sqrt{t}} \qquad (2.5)$$

Thus, the absorption rate is retarded.

Isolated coarser pores that are connected to finer continuous pores cannot become water-filled during a capillary process if they are coarser than about 0,1 μm. This can be easily shown by the geometrical model in Fig 2.1. The coarse spherical pore is connected to finer pores by a narrow bifurcation pore. The model is a good representation of an isolated airpore in a web of fine capillary pores in a cement paste.

When the water front in pore 1 reaches the coarse pore the capillary pressure, which is inversely proportional to the radius of the water meniscus, must be reduced if water should enter the coarse pore. The capillary pressure in the bifurcation pore 2 is however maintained on the high level. Therefore the bifurcation pore immediately sucks water from the coarse pore. The meniscus will therefore not be able to enter the coarse pore. It will remain at its entrance. When the bifurcation pore is full, the fine pore 3 starts to fill by sucking water both downwards and upwards. The coarse pore will continue to be air-filled as long as the capillary pressure is higher in the surrounding fine pore system. An air bubble will therefore be enclosed in the coarse pore.

The air bubble is under pressure; see the next section. Therefore it will be compressed. The relation between the compressed volume V_1 and the initial volume V_o is calculated by Boyle´s law:

$$V_o \cdot P_o = V_1 \cdot P_1 \qquad (2.6)$$

P_o is 10^5 Pa (the ordinary atmospheric pressure). P_1 is given by the Laplace law:

$$P_1 = P_o + 2 \cdot \sigma / r \qquad (2.7)$$

Where σ is the surface tension between water and air (0,074 N/m) and r is the bubble radius.

The volumes V_o and V_1 are:

$$V_o = \frac{4\pi}{3} \cdot R^3 \qquad (2.8)$$

$$V_1 = \frac{4\pi}{3} \cdot r^3 \qquad (2.9)$$

Where R is the radius of the coarse pore.

The ratio of the radii is:

$$r/R = (V_1/V_o)^{1/3} \qquad (2.10)$$

Then, the pressure P_1 is:

$$P_1 = [10^5 + \frac{2\cdot\sigma}{R}\cdot(V_o/V_1)^{1/3}] \qquad (2.11)$$

According to Eq (2.6), the relation between the volume of the compressed bubble and the volume of the spherical pore is:

$$[V_1/V_o]^{1/3}\cdot[V_o/V_1 - 1] = \frac{2\cdot\sigma}{10^5\cdot R} \qquad (2.12)$$

This means that bubbles in smaller pores will immediately become almost totally compressed which is shown by the following example.

Example 2.1:

R= 0,05 µm: V_1/V_o = 0,006 = <1 %

R= 0,10 µm: V_1/V_o = 0,018 = 2 %

R= 1,00 µm: V_1/V_o = 0,32 = 32 %

R= 10 µm: V_1/V_o = 0,87 = 87 %

This means that all pores with diameters smaller than about 0,1 µm are completely compressed and water-filled already during the water absorption process. Larger isolated pores remain air-filled and stay so for shorter or longer time depending on their size and the diffusivity of air through the water-filled pore system. The process of water-filling of the airpores is described in the following section.

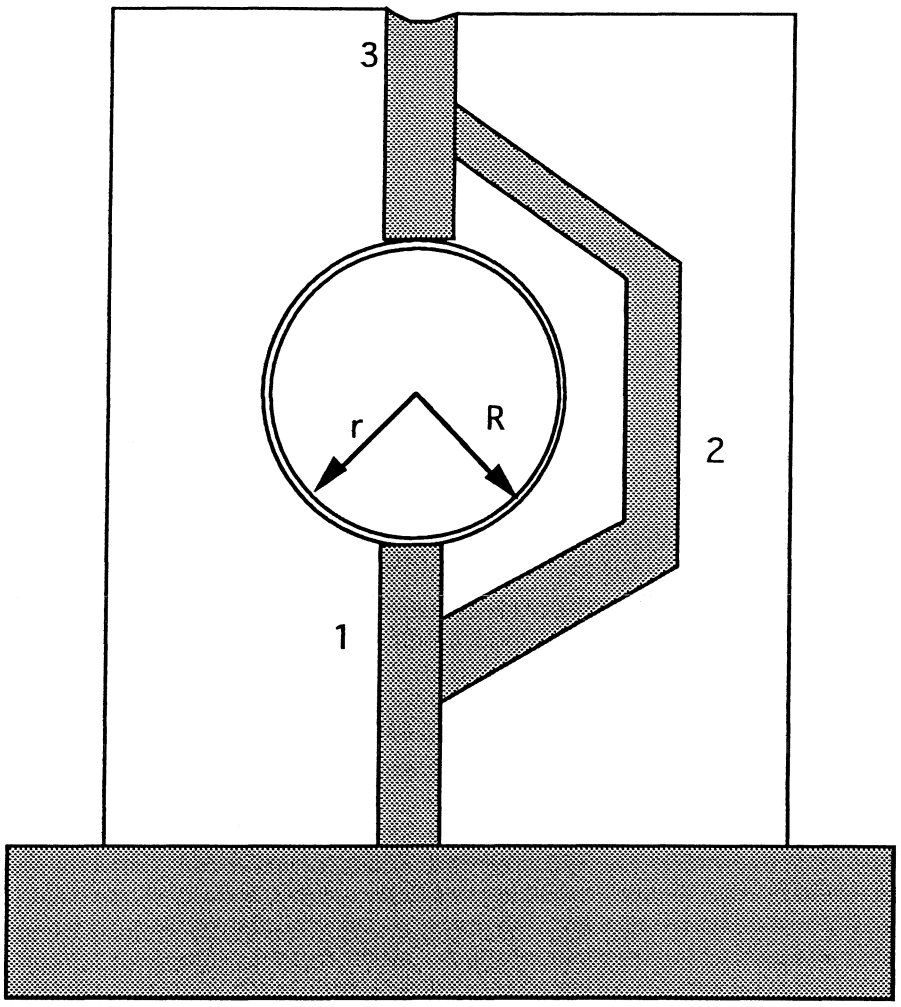

Fig 2.1: Geometrical pore model illustrating the enclosure of airbubbles in coarser pores during a capillary water uptake process.

3. The gradual water absorption in the airpore system

3.1 The basic mechanism

An air bubble, which becomes enclosed in a coarse pore during the capillary water absorption process, is exposed to an internal overpressure ΔP that is inversely proportional to its radius:

$$\Delta P = 2 \cdot \sigma / r \qquad (3.1)$$

where σ is the surface tension air-water and r is the radius of the spherical bubble.

The total pressure is:

$$P = P_o + 2 \cdot \sigma / r \qquad (3.2)$$

Where P_o is the ordinary atmospheric pressure.

The solubility of air in water is proportional to the air pressure. Hence, the bubble will gradually dissolve. Bubbles that are small enough will be dissolved in the pore water surrounding them already a short time after the capillary process ended. The size of these bubbles can be estimated by comparing the amount of air inside the bubble with the water volume needed to dissolve all that air. The total air mass inside a bubble of size r is:

$$m = \rho_1 \cdot \frac{4}{3} \cdot \pi r^3 \qquad (3.3)$$

Where ρ_1 is the density of the compressed air. This is directly proportional to the pressure of the air. Hence,

$$\rho_1 = \rho_o \cdot \frac{P_o + 2 \cdot \sigma / r}{P_o} \qquad (3.4)$$

Where ρ_o is the density of air at 1 atm. ρ_o = 1,25 kg/m^3 at +10°C; see APPENDIX 4. The "extra" solubility Δs of air in water which has become pre-saturated with air at the normal atmospheric pressure is:

$$\Delta s = 3 \cdot 10^{-2} \cdot \Delta P / P_o \text{ kg/m}^3 \qquad (3.5)$$

Where $3 \cdot 10^{-2} / P_o$ is the solubility of air at pressure 1 Pa and 10°C; see APPENDIX 4. This extra solubility due to the increased pressure can be used for dissolving air in the bubble. By

inserting Eq (3.1), (3.4) and (3.5) in eq (3.3) it is possible to calculate the water volume V_w needed in order to dissolve all air in the bubble of size r:

$$V_w = \frac{4 \cdot \pi}{3} \cdot 42 \cdot [1 + P_o/\Delta P] \cdot r^3 \qquad (3.6)$$

The porosity of the cement paste shell surrounding the bubble is of the order of size 40 to 60 %. The cement paste volume needed in order to take care of the dissolved air is therefore about twice as large as the volume given by eq (3.6). Thus, the thickness t (m) of the cement paste shell needed in order to rapidly dissolve an air bubble at +10°C is:

$$t=\{[1+2 \cdot 42 \cdot (1+P_o/\Delta P)]^{1/3}-1\} \cdot r = \{[1+84(1+6,8 \cdot 10^5 \cdot r)]^{1/3}-1\} r \qquad (3.7)$$

The average spacing between airpores is probably shorter the smaller the bubble. An average spacing of 100 μm is assumed. This means that t≈50 μm. Then, according to eq (3.7) bubbles with a radius of about 7 μm will dissolve rapidly at +10 °C. At other temperatures the air solubility is different; see APPENDIX 4. For the temperatures 0 °C and +20 °C the coefficient 42 in eq (3.6) and (3.7) is changed to 33 and 52 respectively. This does, however, not change the size of the rapidly dissolved bubble very much.

Coarser bubbles will not dissolve directly but will stay air-filled for a long time. Air will disappear only gradually due to diffusion through the pore water to larger pores or to the surface. Due to this diffusion the bubble becomes smaller and smaller making the internal pressure higher The dissolution rate will therefore increase with time. However, since the cross section of diffusion decreases with the reduction of the bubble size, the increase in dissolution rate is not directly proportional to the overpressure. It might even be constant during the whole process; see section 3.4. The dissolved air migrates through the pore water to larger air bubbles having a lower internal pressure and, finally, to the surface of the material. The dissolution rate depends on the diffusivity of air in the pore water and is therefore a function of the water/binder ratio and, since different binders create different pore structures, it is also a function of the type of binder.

Many diffusion processes in concrete can be described by a diffusivity δ (m^2/s) which is a simple function of the w/c-ratio:

$$\delta=k_1 \cdot (w/c)^n \approx k_1 \cdot (w/c)^2 \qquad (3.8)$$

Alternatively, it is a function of the capillary porosity, P_c:

$$\delta= k_2+k_3 \cdot P_c{}^n \approx k_3 \cdot P_c{}^2 \qquad (3.9)$$

k_1, k_2, k_3 and n are empirical coefficients determined by the diffusivity of air in pore water.

The rate of dissolution will also be a function of the length of the diffusion path. Hence, an air bubble that is very close to the surface of the concrete ought to be waterfilled before a similar bubble in the interior of the concrete. The dissolution will, however, not occur as a moving boundary process. Since all bubbles are oversaturated with air, a local dissolution will occur simultanously in the pore water surrounding each bubble. The dissolved air will move to a neighbouring pore with a lower pressure and from there to the next pore and so on. Finally, it reaches the surface. Therefore, due to this inter-bubble diffusion and due to the extremely large number of bubbles, the dissolution will probably occur rather homogeneously within a zone of a certain thickness. This zone is probably considerably thicker than the so called critical thickness which is a measure of the largest material volume which is not harmed by frost even when frozen in a completely water saturated condition. This has been indicated by a simple theoretical calculation in /7/. The critical thickness is only about 0,3 to 0,5 mm for concrete /8/.

Seen over a larger material volume, there will of course be a certain gradient in air concentration in the pore water from the surface of the concrete inwards due to the fact that diffusion to the surface must occur. This requires a gradient. In the normal, practical case, however, it is the outmost millimeters or centimeters of the concrete that is most interesting and this zone can be approximately treated as "non-gradient" zone; at least when it comes to an analysis of the inter-bubble diffusion.

3.2 The global diffusion

The global diffusion rate in the material as a whole will, due to the inter-bubble diffusion, be a function of the air or bubble content. The larger the air content, the lower the inter-bubble spacing and the larger the rate of air-diffusion and water-filling of the bubbles.

The inter-bubble spacing L (m) can be described by the Powers´ equation:

$$L = [3/\alpha_r] \cdot \{1,4[V_p/a+1]^{1/3}-1\} \qquad (3.10)$$

where, α_r is the specific surface of the air-filled part of the bubble system (m^{-1}), V_p is the volume fraction of cement paste (air pores excluded) and a is the air bubble volume as a fraction of the concrete volume.

As a first approximation, the global diffusivity of dissolved air is therefore described by a function of the following type:

$$\delta = \delta_o \cdot \frac{(w/c)^2}{[3/\alpha_r] \cdot \{1,4[V_p/a+1]^{1/3}-1\}} \qquad (3.11)$$

The constant δ_o depends on the fineness of the pore structure. It might be a function of the type of cement and the type of mineral admixture used.

Eq (3.11) is plotted in Fig 3.1. The rate of air diffusion from the air bubbles will increase with increasing air bubble content and increasing w/c-ratio. In the real case a higher air-bubble volume will, however, be favourable since it will take a longer time before the critical distance is exceeded. Hence, the service life is increased; see section 1.2.

In Fig 3.2 the coefficient η describing the slow rate of water absorption during the long term storage of slag cement concretes in water is plotted versus the air content. η is defined by $\Delta S = \eta \cdot \log(\text{time})$ where ΔS is the increase in the total degree of saturation of the concrete. The general shape of the curves are similar to those predicted by eq (3.11) and shown in Fig 3.1; viz. the water absorption rate increases with increasing air content.

The total amount of air Q (kg) transferred over the distance Δx (m) during the time interval Δt (s) is described by:

$$Q = \delta \cdot A \cdot \Delta t \cdot \Delta c / \Delta x \qquad (3.12)$$

Where A is the cross section of flow (m^2) and Δc is the difference in concentration of dissolved air (kg/m^3) over the distance Δx.

The concentration gradient Δc is according to Henry´s law proportional to the gradient in air pressure and therefore, according to eq (3.1) and seen over a larger material volume and cross section, approximately inversely proportional to the gradient in the "average size" r_m of the remaining air bubbles over the distance Δx.

$$\Delta c = \text{constant} \cdot \sigma [1/r_{m,1} - r_{m,2}] \qquad (3.13)$$

Where $r_{m,2}$ and $r_{m,1}$ are the "average bubble radii" at distance x and and x+Δx from the surface. The "average bubble radius" is the radius of a fictive bubble staying in equilibrium with the air concentration of the surrounding pore water. The constant in eq (3.13) describes the relation according to Henry´s law between air pressure and dissolved air. For the concentration difference of dissolved air between the free concrete surface and the pore water inside the concrete on the distance Δx from the surface the following expression is valid:

$$\Delta c = \text{constant} \cdot \sigma / r_{m,1} \qquad (3.14)$$

The cross section A for the global diffusion is as a first approximation considered to be directly proportional to the volme

fraction of the sum of capillary pores and air bubbles in relation to the total cement paste volume, air bubbles included. Thus, the fine gel pores are not supposed to take part in the diffusion of air. Then A is:

$$A = \frac{w/c-0,39\cdot\beta+a\cdot 1000/c}{w/c+0,32+a\cdot 1000/c} \qquad (3.15)$$

Where β is the degree of hydration and a is the volume of air bubbles (m^3) in 1 m^3 of the concrete. No consideration is taken to the interfaces between aggregate grains and cement paste. They do certainly also have an effect on the diffusivity.

With this equation and eq (3.13) or eq (3.14) inserted in eq (3.12) the total air transport over the distance Δx in 1 m^2 of the concrete cross section can be estimated. A general equation for this global diffusion is:

$$q= -\delta\cdot d^2c/dx^2 \qquad (3.16)$$

Where q is the flux of dissolved air ($kg/m^2\cdot s$).

The main problem in using this general equation or the numerical eq (3.12) is that is difficult to estimate the concentration gradient dc/dx. Probably, however, as said above in 3.1, it is not always necessary to deal with the global diffusion since most of the water absorption in the bubbles occur due to local inter-bubble diffusion between neighbouring bubbles. This diffusion goes from smaller to larger bubbles.

3.3 The local diffusion between neighbouring air bubbles - principles

Let us consider two neighbouring bubbles with the radii r_1 and r_2 ($r_1<r_2$). Directly after the capillary uptake has ceased the radii of the bubble mensci in the pores are $r_{1,o}$ and $r_{2,o}$.

According to Boyle´s law those radii are:

$$r_i=\{r_{i,o}^2[r_{i,o}+2\cdot\sigma/P_o]\}^{1/3} \qquad (3.17)$$

where i stands for either 1 or 2. $r_{i,o} \rightarrow r_i$ for large values of r_i

Diffusion starts from pore 1 to pore 2. The air volume in pore 1 diminishes and the air volume in pore 2 increases. After a certain time the new radii are $r_{1,t}$ and $r_{2,t}$.

The initial air masses in pore 1 and 2 are m_1 and m_2 where $m_1/m_2=[r_1/r_2]^3$. After a certain time of diffusion $\gamma\cdot m_1$ is lost from pore 1 and transferred to pore 2. Then Boyle´s law gives:

Pore 1:

$$P_o+2\sigma/r_{1,o}=\{P_o+2\sigma/r_{1,t}\}\cdot\{r_{1,t}/r_{1,o}\}^3\cdot 1/(1-\gamma) \qquad (3.18)$$

Pore 2:

$$P_o+2\sigma/r_{2,o}=\{P_o+2\sigma/r_{2,t}\}\cdot\{r_{2,1}/r_{2,0}\}^3\cdot 1/[1+(r_1/r_2)^3\cdot\gamma] \qquad (3.19a)$$

Air continues to flow to pore 2 even after all water that was initially contained in it has been displaced. The increased pressure in pore 2 is taken care of by curved menisci in the entrance to capillaries leading into pore 2. After this has happened the following relation is valid for pore 2:

$$\text{Pore 2: } P_o+2\sigma/r_{2,o}=P_{2,t}\cdot\{r_2/r_{2,0}\}^3\cdot 1/[1+(r_1/r_2)^3\cdot\gamma] \qquad (3.19b)$$

The pressures in the bubbles are:

$$\text{Pore 1: } P_1= P_o+2\sigma/r_{1,t} \qquad (3.20)$$

$$\text{Pore 2: } P_2= P_o+2\sigma/r_{2,t} \quad \text{for } r_{2,t}<r_2 \qquad (3.21a)$$

$$P_2= P_{2,t} \quad \text{for } r_{2,t}=r_2 \qquad (3.21b)$$

Air will flow from pore 1 until the pressure in pore 2 equals the pressure in pore 1. This condition is only valid when all water in pore 2 has been displaced. Before that, a transfer of air from pore 1 to pore 2 will always lead to a higher pressure increase in pore 1 than in pore 2 leading to a continued flow. By equaling eq (3.18) and (3.19b) one obtains the following equation for the maximum fraction of air that can flow from pore 1 to pore 2:

$$\gamma < \left[\frac{P_o+2\sigma/r_{1,t}}{\{P_o+2\sigma/r_{2,o}\}\{r_{2,o}/r_2\}^3} - 1\right]\{r_2/r_1\}^3 \qquad (3.22)$$

Where $r_{1,t}$ is a function of γ. From eq (3.18) the following relation between $r_{1,t}$ and γ obtained:

$$P_o\cdot r_{1,t}^3+2\sigma\cdot r_{1,t}^2=r_{1,o}^3\{P_o+2\sigma/r_{1,o}\}\{1-\gamma\} \qquad (3.23)$$

This equation must be solved numerically.

The initial bubble radii $r_{1,o}$ and $r_{2,o}$ in eq (3.22) and (3.23) are functions of the pore sizes r_1 and r_2. The relations is given in eq (3.17).

Eq (3.22) shows that there is a maximum amount of air that can flow from pore 1 to pore 2. This amount is a function of the relative pore size (r_1/r_2) and a function of the absolute pore sizes (r_1 and r_2). It is clear from eq (3.22) that the amount of air that can flow from a smaller to a larger bubble increases with increased size ratio between the two bubbles.

The volume changes of the bubbles are:

Pore 1: $\Delta V_1 = -\{r_{1,o}^3 - r_{1,t}^3\} \cdot 4 \cdot \pi/3$ (3.24)

Pore 2: $\Delta V_2 = +\{r_{1,t}^3 - r_{1,o}^3\} 4 \cdot \pi/3$ for $r_{2,t} < r_2$ (3.25a)

$\Delta V_2 = +\{r_2^3 - r_{1,o}^3\} 4\pi/3$ for $r_{2,t} = 0$ (3.25b)

The net volume change is:

$$\Delta V = \Delta V_1 + \Delta V_2 \quad (3.26)$$

The pressure in pore 1 will, at the start, always be higher than in pore 2. When the pores are small the pressure in pore 1 maintains a higher value even when all water in pore 2 has been displaced by the air arriving. Small bubbles will therefore vanish completely as is seen in example 3.1 below. Air from small pores can move to pores of almost all sizes without being stopped by too large a pressure increase in the larger pores. Air in larger pores, on the other hand, cannot be transferred to pores that are not very much larger since the pressure in the latter will soon reach the driving pressure in the smaller pore. This is shown by example 3.2 below. Large pores can, however be completely emptied to pores that are very much larger; see example 3.3 below.

The volume changes and the pressures are best shown by three numerical examples:

Example 3.1; Small pores: r_1=10 μm; r_2=20 μm.

Eq (3.17) gives:

$r_{1,o}$=9,53 μm, $r_{2,o}$=19,51μm.

Pore 1: Eq (3.18), (3.20) and (3.24) give:

γ=0,25: $r_{1,t}$=8,62 μm. $P_{1,t}=1,17 \cdot 10^5$ Pa. $\Delta V_1 = -0,94 \cdot 10^{-15}$ m^3

γ=0,50: $r_{1,t}$=7,47 μm. $P_{1,t}=1,20 \cdot 10^5$ Pa. $\Delta V_1 = -1,88 \cdot 10^{-15}$

γ=0,75: $r_{1,t}$=5,84 μm. $P_{1,t}=1,25 \cdot 10^5$ Pa. $\Delta V_1 = -2,79 \cdot 10^{-15}$

γ=1,00. $r_{1,t}$=0 $P_{1,2}=\infty$ $\Delta V_1 = -3,62 \cdot 10^{-15}$

Pore 2: Eq (3.19), (3.21) and (3.25) give:

γ=0,25: $r_{2,t}$=19,71 μm. $P_{2,t}=1,08 \cdot 10^5$ Pa. $\Delta V_2 = +0,97 \cdot 10^{-15}$m^3

γ=0,50: $r_{2,t}$=19,92 μm. $P_{2,t}=1,07 \cdot 10^5$ Pa. $\Delta V_2 = +2,00 \cdot 10^{-15}$

γ=0,75: $r_{2,t}$=20 μm. $P_{2,t}=1,09 \cdot 10^5$ Pa. $\Delta V_2 = +2,40 \cdot 10^{-15}$

γ=1: $r_{2,t}$=20 μm. $P_{2,t}=1,12 \cdot 10^5$ Pa. -"- -"-

The net volume reductions are:

γ=0,25: $\Delta V = +0,03 \cdot 10^{-15}\ m^3$
γ=0,50: $\Delta V = +0,12 \cdot 10^{-15}$
γ=0,75: $\Delta V = -0,39 \cdot 10^{-15}$
γ=1: $\Delta V = -1,22 \cdot 10^{-15}$

Thus, the pressure is always higher in bubble 1.Therefore, this will vanish completely. There is a small increase in volume as long as water in pore 2 is under displacement by the air flowing into it. The reason is that the pressure is lower in pore 2. When all water in pore 2 is displaced there is, however, a decrease in volume as the bubble 1 dissolves which means that water must be sucked into the bubble system from an exterior source. This explains why water is absorbed in air-entrained concrete that is stored for a long time in water. It can be noted that the maximum volume contraction is only $1,22 \cdot 10^{-15}/3,62 \cdot 10^{-15}$=33 % of the initial volume of the dissolved bubble 1. The volume contraction should have been larger had air been transferred to a smaller bubble; e.g. when the radius of pore 2 is 15 µm the maximum volume reduction due to transfer of air from pore 1 is 65 % of the dissolved volume.

Example 3.2; Larger pores with small size ratio:
r_1=100 µm. r_2=200 µm

Eq (3.17) gives:

$r_{1,o}$=99,51 µm, $r_{2,o}$=199,50 µm

Pore 1:

γ=0,25: $r_{1,t}$=90,3 µm. $P_{1,t}=1,016 \cdot 10^5$ Pa. $\Delta V_1=-1,043 \cdot 10^{-12}\ m^3$
γ=0,50: $r_{1,t}$=78,9 µm. $P_{1,t}=1,019 \cdot 10^5$ Pa. $\Delta V_1=-2,069 \cdot 10^{-12}$
γ=0,75: $r_{1,t}$=62,5 µm. $P_{1,t}=1,024 \cdot 10^5$ Pa. $\Delta V_1=-3,103 \cdot 10^{-12}$
γ=1: $r_{1,t}$=0. $P_{1,t}$ trivial. $\Delta V_1=-4,125 \cdot 10^{-1}$

Pore 2:

γ=0,25: $r_{2,t}$=200 µm. $P_{2,t}=1,031 \cdot 10^5$ Pa. $\Delta V_2=0,25 \cdot 10^{-12}\ m^3$
γ=0,50: -"- $P_{2,t}=1,062 \cdot 10^5$Pa. -"-
γ=0,75: -"- $P_{2,t}=1,094 \cdot 10^5$Pa. -"-
γ=1: -"- $P_{2,t}=1,125 \cdot 10^5$Pa. -"-

The pressure will be higher in pore 2 than in pore 1 already before 25 % of the air in the latter has been recieved. Therefore, air transfer stops already when a small fraction of the air in pore 1 has been transferred.

The ΔV_2-values for pore 2 corresponds to the displacement of water in pore 2 due to inflowing air before the increased pressure in pore 2 stops the process.

Example 3.3; Larger pores with large size ratio:
r_1=100 μm, r_2=400 μm

Eq (3.17) gives:

$r_{1,o}$=99,51 μm. $r_{2,o}$=399,50 μm

Pore 1:

The same values of $r_{1,t}$, $P_{1,t}$ and ΔV_1 as for example 3.2 are valid.

Pore 2:

γ=0,25: $r_{2,o}$=400 μm. $P_{2,t}=1,004\cdot10^5$ Pa. $\Delta V_2=+1,004\cdot10^{-12}$ m^3
γ=0,50: -"- $P_{2,t}=1,008\cdot10^5$Pa. -"-
γ=0,75: -"- $P_{2,t}=1,012\cdot10^5$Pa. -"-
γ=1: -"- $P_{2,t}=1,015\cdot10^5$Pa. -"-

In this case the pressure is always higher in pore 1. Therefore, the bubble 1 will vanish.

The total volume reduction due to air transfer is:

γ=0,25: $\Delta V=-0,04\cdot10^{-12}$ m^3
γ=0,50: $\Delta V=-1,07\cdot10^{-12}$
γ=0,75: $\Delta V=-2,10\cdot10^{-12}$
γ=1: $\Delta V=-3,12\cdot10^{-12}$

Thus there is a gradual decrease in volume. The total volume reduction when bubble 1 has disappeared is $3,12\cdot10^{-12}/4,12\cdot10^{-12}$=75 % of the initial volume of the dissolved bubble 1.

The analysis performed above shows that there is a complicated network of local exchanges of air from smaller to adjacent larger bubbles. Besides, air that is displaced from one pore to a neighbouring larger pore will soon leave this for a still larger pore and so on. This process can hardly be described by other than statistical methods or computer simulations assuming a random distribution in space of the spherical air pores. It is quite clear, however that there is a gradual coarsening of the remaining bubble system; the smallest bubbles being lost at first. Only after a very long time are the biggest bubbles lost.

It is also quite clear that there would be a gradual water-fil

ling of bubbles even if there were no diffusion at all of air from those dissolved bubbles to the surface of the concrete. On the contrary, there must be a diffusion of water **from** the surface to the interior of the concrete. This depends on the fact that there is a net volume reduction when air is dissolved and transferred to larger bubbles. This water uptake due to numerous local air transfers occuring simultaneously over the entire concrete body explains the observation that the long term absorption in concrete stored in water seems to be independent of the thickness of the specimen as long as this is not too large, /7/. This also means that the gradient in air concentration of the pore water from the interior to the surface might be rather small even in cases where a large amount of the smallest air bubbles are lost due to dissolution and water absorption. In the long run, however, when also the largest bubbles are lost, there must be a global gradient in concentration of dissolved air towards the surface.

The driving potential for diffusion of dissolved air from pore to pore is rather small, especially for the largest bubbles. For a pore system, as that treated in example 3.3, the air-pressure gradient is only about 1000 Pa leading to a gradient in dissolved air of about $2,5 \cdot 10^{-4} kg/m^3$ which is only 1 % of the the amount of dissolved air at normal pressure. Of course, the gradient is larger for smaller bubbles.

3.4 The local diffusion between neighbouring pores - calclculation method

The rate of the local diffusion between neighbouring pores can be determined by eq (3.12) if reasonable values of the concentration difference Δc, the cross section of flow A and the inter-pore spacing Δx are inserted.

For the inter-pore diffusion between a small bubble with radius $r_{1,o}$ and an adjacent larger bubble with radius $r_{2,o}$ the concentration difference is according to eq(3.5):

$$\Delta c = s \cdot 2\sigma[1/r_{1,o} - 1/r_{2,o}] \cdot \beta \quad kg/m^3 \qquad (3.27)$$

Where s is the solubility of air in water. It is $2,4 \cdot 10^{-7} kg/m^3$ at +20°C and 1 Pa. β is a correction factor that takes care of the changes in the air pressure in the pores caused by the air transfer, viz. the initial pressures $2\sigma/r$ will not be maintained. β is a function of the pore sizes. For large pores β=1. For small pores it is about 2.

The effective cross section of flow A is

$$A = \pi \cdot r_1 \cdot r_2 \qquad (3.28)$$

The reason why the pore radii r_1 and r_2 have been inserted and

not the bubble radii $r_{1,o}$ and $r_{2,o}$ is that the diffusion of air through the water phase inside the relatively coarse airpore is supposed to be much more rapid than the diffusion through the dense capillary pore system.

The inter-bubble spacing is L. Then, the total air flow is:

$$Q=\delta\cdot\Delta t\cdot\pi\cdot r_1\cdot r_2\cdot s\cdot 2\sigma[1/r_{1,o}-1/r_{2,o}]\cdot\beta/L \quad [kg] \qquad (3.29)$$

The diffusivity $\delta[m^2/s]$ of air in hardened cement paste is not very well known. For air in bulk water at +25 °C it is $2\cdot10^{-9}$ m^2/s. In cement paste it is probably decreased by a factor 100 or even more. A value of 10^{-11} m^2/s is selected. The distance L between pores varies from pore to pore. An average value of 300 μm is selected. This is probably a bit too high for small bubbles but a bit too small for large bubbles. The surface tension σ is 0,074 N/m.

When those values and the solubility of air are inserted the following expression is obtained:

$$Q=3,9\cdot10^{-15}\cdot r_1\cdot r_2\cdot[1/r_{1,o}-1/r_{2,o}]\cdot\beta\cdot\Delta t \quad [kg] \qquad (3.30)$$

This equation can be used for a rough estimate of the time needed to epmty a pore. The same examples as above (examples 3.1 and 3.2) are used.

Example 3.4 (See example 3.1): r_1=10 μm; r_2=20 μ m.

The total amount of air in pore 1 is:

$$Q=1,25\cdot4\cdot\pi\cdot(10\cdot10^{-6})^3/3 = 5,23\cdot10^{-15} \quad [kg]$$

Where 1,25 kg/m^3 is the density of air at +10 °C.

The coefficient β is about 2 (see the previous solution).

$r_{1,o}\approx r_1$; $r_{2,o}\approx r_2$ (see above)

Insertion in eq (3.30) gives:

$$5,23\cdot10^{-15}=3,9\cdot10^{-15}\cdot10\cdot10^{-6}\cdot20\cdot10^{-6}[1/10\cdot10^{-6}-1/20\cdot10^{-6}]\cdot2\cdot\Delta t$$

The time needed to empty pore 1 is: **Δt=18,5 hours.**

Example 3.5 (see example 3.3); r_1=100 μm, r_2=400 μ m:

The total amount of air in pore 1 is:

$$Q=1,25\cdot4\cdot\pi(100\cdot10^{-6}\}^3/3 = 5,23\cdot10^{-12} \quad [kg]$$

The coefficient β is about 1.

Insertion in eq (3.30) gives:

$5{,}23 \cdot 10^{-12} = 3{,}9 \cdot 10^{-15} \cdot 100 \cdot 10^{-6} \cdot 400 \cdot 10^{-6} [1/100 \cdot 10^{-6} - 1/400 \cdot 10^{-6}] \cdot \Delta t$

The time needed to empty pore 1 is: **Δt = 1240 hours = 52 days.**

If the diffusivity was only 10^{-12} m^2/s, which is quite possible, the times needed should be increased by a factor 10 to 8 days and 520 days respectively. However, according to eq (3.30) there is a direct proportionality between the size of the recipient bubble and the time needed to empty the smaller bubble. Therefore the times should have been somewhat shorter had the recipent bubbles been larger than the values 20 μm and 400 μm assumed in the examples.

The calculation indicates that the time to fill the airpore system is quite long, especially for dense concretes and/or concretes with coarse air-bubble systems. Airpore systems that are very fine will, however, rapidly become inactivated by water. In the examples above it takes about 70 times as long time to empty a bubble contained in a pore with radius 100 μm as a bubble in a pore with radius 10 μm. Their volume ratio is however 1000. The time needed is evidently not proportional to the volumes. This mainly depends on the fact that the cross section of diffusion increases with the bubble size at the same time as the length of the diffusion path has been supposed to be constant. Besides, the size ratio between pore 1 and 2 is twice as large in example 2 further increasing the cross section.

A complication with eq (3.29) is that the bubble size in pore 1 decreases as air is leaving ; it changes from $r_{1,o}$ to $r_{1,t}$. Therefore, the over-pressure in pore 1 increases with time. This is, however, approximately taken care of by the coefficient β. Besides, the effective cross section of air flow becomes a bit lower than the value $\pi \cdot r_1 \cdot r_2$ assumed in eq (3.29). The net effect probably is that the flow from pore 1 is relatively constant during the whole process and fairly well described by eq (3.29). The complication is avoided in the model which will now be described.

In the real material, diffusion does not take place between individual pores as calculated above. There will be a sort of average local diffusion governed by a diffusivity that is a function of the w/c-ratio and the air content. A diffusivity of the type shown in eq (3.11) could perhaps be used. The value δ_o is not known. It might be estmated from measurements of saturated gas flow through water-saturated concrete. It is supposed to be the same for diffusion from all pores.

Further on, the radius r_2 is supposed to be infinite corresponding to a free water surface or to the meniscus in a pore that is very much larger than r_1. Diffusion is supposed to be symmetrical within a material sphere surrounding the bubble. The

radius of this sphere, or the length of the flow path, is L.

Then, the general equation for the flux of air q´ [kg/s] from a bubble with radius r_1 is:

$$q' = \delta \cdot \frac{(L+r_1)\, r_{1,t} \cdot 4\pi}{L} \cdot \Delta c = \delta \cdot \frac{(L+r_1)\, r_1 \cdot 4\pi}{L} \cdot s \cdot 2\sigma / r_{1,t} \qquad (3.31a)$$

Or:

$$q' = \delta \cdot \frac{(L+r_1) \cdot 4\pi}{L} \cdot s \cdot 2\sigma \qquad (3.31b)$$

Where δ is the bulk diffivity of air in pore water; s is the solubilty of air. It is $2{,}4 \cdot 10^{-7}$ [kg/(m^3·Pa)] at a pressure of 1 Pa and +20°C. In eq (3.31) it is assumed that the resistance to diffusion is just as high in the absorbed water phase inside pore 1 as in the cement paste.

It is reasonable to assume that the diffusion path increases with increasing size of the bubble being emptied; c.f. eq (3.10), which shows that there is an inverse proportionality between the specific surface of the pore and the average spacing provided the total bubble volume under consideration is constant. The following assumtion is made:

$$L = \varepsilon \cdot r_1 \quad \text{where } \varepsilon > 1 \qquad (3.32)$$

Thus, the diffusion path increases linearily with the bubble size. Then, eq (3.31) can be written:

$$q' = \delta \cdot [1+1/\varepsilon] \cdot 4\pi \cdot s \cdot 2\sigma \qquad \text{[kg/s]} \qquad (3.33)$$

The rate of flow of air from a certain bubble is therefore approximately independent of its size and only dependent of the ratio of the pore size to the length of the diffusion path. The application of eq (3.33) is shown by two examples. The diffusivity is supposed to be 10^{-11} m^2/s. The coefficient $\varepsilon = 5$.

Thus, $q' = 5{,}6 \cdot 10^{-18}$ [kg/s]

Example 3.6: Pore radius 10 µm. L = 5·10 = 50 µm

The total amount of air (see above) = $5{,}23 \cdot 10^{-15}$ [kg]

The time required = **0,25 hours**.

Example 3.7: Pore radius 100 µm. L = 500 µm.

The total amount of air = $5{,}23 \cdot 10^{-12}$ [kg]

The time required = 259 hours = **11 days**.

The time required is directly proportional to the bubble volume. Eq (3.33) implies that the rate of air flow from a bubble in kg per second is independent of the bubble size. It is a constant which is only a function of the bulk diffusivity δ, the ratio of diffusion path to the bubble radius ε, the solubility of air in water, s, and the surface tension σ:

$$\mathbf{q' = constant_1 \quad [kg/s]} \qquad (3.34)$$

It might be that the diffusivity in the water phase inside pore 1 is much higher than the diffusivity in the cement paste. In such a case eq (3.33) is modified to:

$$q' = \delta[1+1/\varepsilon] \cdot r_1 \cdot 4\pi \cdot s \cdot 2\sigma / r_{1,t} \qquad (3.35)$$

This equation is much more difficult to handle since it implies that the rate of water-filling of the airpore is not a constant but a function of the actual degree of saturation of the pore. It must be solved numerically. For the smallest airpores, at least, eq (3.33) and (3.34) can be used without too much error. For those pores, which are also the most important for frost resistance, the diffusion path outside the pore is much larger than the diffusion path inside the pore. Besides, most of the airpore volume is filled before the difference between the pore radius r_1 and the bubble radius $r_{1,t}$ is very large; c.f Examples 3.1 and 3.2 above.

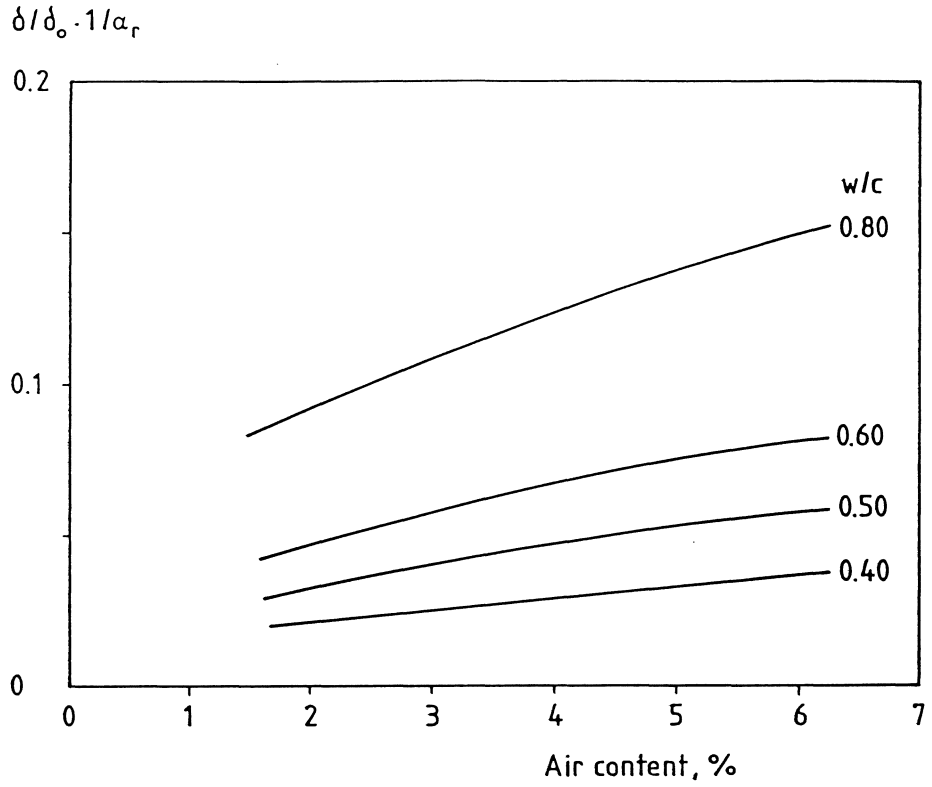

Fig 3.1: Theoretical effect of the w/c-ratio and air content on the diffusivity of dissolved air through the pore water; eq (3.10) and (3.11). The amount of mixing water is supposed to be 180 kg/m^3 in all mixes.

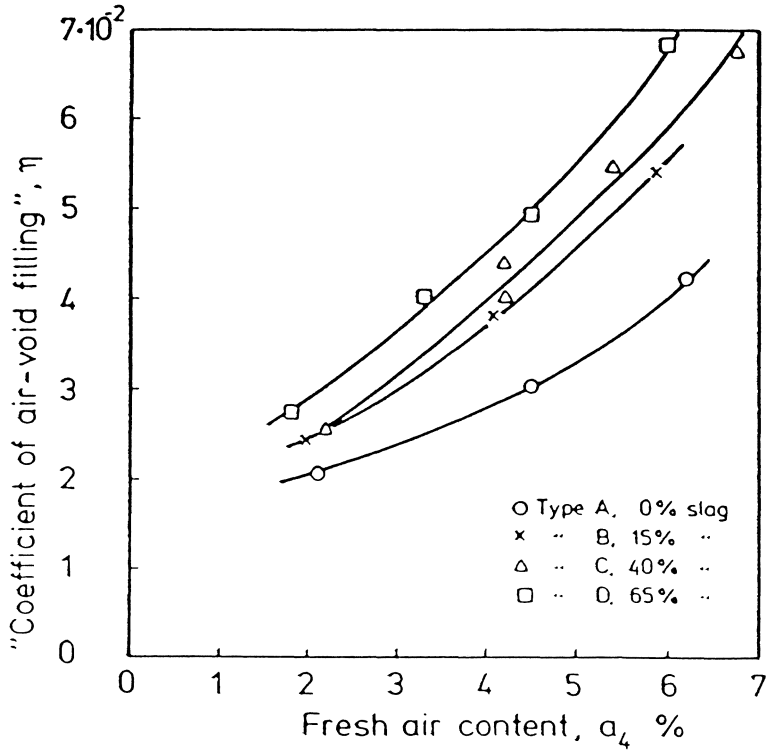

Fig 3.2: Experimentally determined rates of the water absorption during 30 days in concretes made with slag cements and varying air content; /8/. The "coefficient of air-void filling", η. It is defined by the relation $\Delta S = \eta \cdot \log(\text{time of water storage})$.

4. The water absorption in model air-pore systems

4.1 Introduction

In a real air pore system there are air-bubbles of all sizes varying from about 5 μm to 500 μm or more. Therefore, the simple solution performed above in which only a two-bubble system is regarded is too simplified. Such an analysis does however show that air will be transferred from every pore irrespectively of its size to larger pores in the neighbourhood. Certainly, the pore will also recieve air from smaller adjacent pores. This is the case especially for the largest pores. Therefore it might be a certain delay before the pore will be "a net exporter" of air which will migrate to larger pores still, or to the surface. Two different models for a description of this water-filling process is treated below:

Model 1: It is assumed that every pore starts to absorb water already when the capillary process is ended in its surroundings. The rate of air diffusion from a pore expressed in terms of kg per second and the rate of water-filling of a pore is supposed to be the same for all pores; c.f. eq (3.34). Thus, a smaller pore is always completely filled before a larger one, but the water absorption is going on simultaneously in all pores. This model implies that the total water content in the airpore system is not only distributed among the smallest pores but that all air-pores contain more or less water. Model 1 is a non-equilibrium model; the total free energy of the air-water system is higher than in Model 2.

A graphical representation of Model 1 is shown in Fig 4.1.

Model 2: The net diffusion process between all airpores in the system is such that a coarser pore will not start to take up water until the next smaller pore is completely water-filled. This model implies that the total water content in the airpore system is only distributed among the smallest pores while the coarser part of the pore system is completely air-filled (apart from a thin water meniscus along the periphery). Model 2 is the most plausible model from a thermodynamical point of view since it corresponds to the lowest free energy level of the system.

A graphical representation of Model 2 is shown in Fig 4.2.

4.2 Model 1: Absorption in all bubbles simultaneously

4.2.1 Theory

Let us consider an airpore distribution curve f(r); see Fig 1.2. This distribution could be just a mathematical expression describing the shape of the real distribution curve but not the absolute level of this. A fictitious airpore volume V_a' calculated by this distribution is:

$$V_a' = \int_{\approx 10\ \mu m}^{\infty} \frac{4\pi}{3} \cdot r^3 \cdot f(r) \cdot dr \qquad [m^3] \qquad (4.1)$$

The lower limit 10 μm is supposed to be the smallest pore that is not water-filled already during the capillary process.

The real distribution F(r) is found by utilizing the real airpore volume V_a:

$$V_a = \int_{\approx 10\ \mu}^{\infty} \frac{4\pi}{3} \cdot r^3 \cdot F(r)\ dr \qquad [m^3] \qquad (4.2)$$

The relation between the two distributions is:

$$F(r) = f(r) \cdot V_a / V_a' \qquad (4.3)$$

In the following f(r) is used.

The average pore radius $r_{m,i}$ in the interval Δr is defined:

$$r_{m,i} = (r_i + r_{i+1})/2 \qquad [m] \qquad (4.4)$$

The initial volume of air in one bubble of this size is:

$$V_1(r_{m,i}) = \frac{4\pi}{3} \cdot (r_{m,i})^3 \qquad [m^3] \qquad (4.5)$$

The initial weight of this air is:

$$Q_1(r_{m,i}) = V_1(r_{m,i}) \cdot \rho_o \qquad [kg] \qquad (4.6)$$

Where ρ_o is the density of air at normal pressure and at the actual temperature.

The number of pores with radius $r_{m,i}$ in the interval Δr is:

$$\Phi(r_{m,i}) = f(r_{m,i}) \cdot \Delta r \qquad (4.7)$$

The initial volume of air in all those bubbles is:

$$V'(r_{m,i}) = \Phi(r_{m,i}) \cdot \frac{4}{3} \cdot \pi \cdot r_{m,i}^3 \quad [kg] \qquad (4.8)$$

The time needed to completely empty each one of these bubbles is:

$$t(r_{m,i}) = Q_1(r_{m,i})/q' = \frac{\rho_o}{q'} \cdot \frac{4\pi}{3} \cdot r(_{m,i})^3 \quad [s] \qquad (4.9)$$

Where q´is the rate of air diffusion from the bubble in kg/s. q´is a function of the diffusivity of the cement paste but not of the bubble size; see eq (3.31). Therefore, it depends on the total airpore volume, the w/c-ratio the type of binder etc; see eq (3.11). The time needed to empty an air bubble is directly proportional to the bubble volume.

The time process of air diffusion is schematically shown in Fig 4.1. The total air volume that has diffused in the concrete during the time 0 to $t(r_{m,1})$ corresponding to the time it takes to completely fill the smallest bubbles ($r_{m,1}$) is:

$$V'_1 = t(r_{m,1}) \cdot \{ \frac{V'(r_{m,1})}{t(r_{m,1})} + \frac{V'(r_{m,2})}{t(r_{m,2})} + \ldots\ldots\ldots\ldots + \frac{V'(r_{m,n})}{t(r_{m,n})} \} \quad [m^3] \qquad (4.10)$$

The total amount of air that has diffused after time $t(r_{m,i})$ is:

$$V'_i = V'(r_{m,1}) + V'(r_{m,2}) + \ldots + V'(r_{m,i-1}) + t(r_{m,i}) \cdot \{ \frac{V'(r_{m,i})}{t(r_{m,i})} + \ldots\ldots\ldots + \frac{V'(r_{m,n})}{t(r_{m,n})} \} \qquad (4.11)$$

The total volume of air transported from the air bubbles, V'_i is evidently a time function; $V'_i = V'[t(r_{m,i})] = V'(t)$.

After a very long time the total airpore system is water-filled. Then, the volume of air that has diffused equals the total initial air content in the airpore system V_a':

$$V'_n = V'(r_{m,1}) + V'(r_{m,2}) + \ldots\ldots + V'(r_{m,n}) = V'_a \quad [m^3] \qquad (4.12)$$

The real volume of air transferred in the real airpore system

is obtained by multiplying eq (4.10), (4.11) and (4.12) by the factor V_a/V'_a where V_a is the real airpore volume; see eq (4.3).

The water volume $V_w'(t)$ that has been taken up by the material at time t of diffusion is supposed to be equal to the volume at normal pressure of diffused air $V'(t)$:

$$V_w'(t) = V'(t) \qquad [m^3] \tag{4.13}$$

The mass of water taken up at time t is:

$$W_w'(t) = V_w'(t) \cdot 1000 \qquad [kg] \tag{4.14}$$

The degree of water-filling at time t, or the "real" degree of saturation $S_a(t)$, of the entire airpore system is:

$$S_a(t) = V_w'(t)/V_a' \qquad [m^3/m^3] \tag{4.15}$$

The **"effective" degree of saturation** $S_a(t_j)_{eff}$ after time $t_j = t(r_{m,j})$ is defined as the degree of saturation when only water in completely water-filled airpores, i.e. pores with radii smaller than $r_{m,j}$, is considered. The effective degree of saturation is

$$S_a(t_j)_{eff} = \frac{\sum_1^j V'_i}{V_a'} = \frac{\sum_1^j V'_i}{V_w'(t_j)} \cdot S_a(t_j) \tag{4.16}$$

The effective degree of saturation can also be obtained analytically from the airpore distribution. The volume $V_{w,i}'$ of totally water-filled pores with radii smaller than $r_i(\mu m)$ is:

$$V_{w,i}' = \int_{\approx 10}^{r_i} \frac{4\pi}{3} \cdot r_i^3 \cdot f(r) \cdot dr \tag{4.17}$$

The radius can be substituted by the corresponding time t_i to fill completely the pore with radius r_i. Eq (4.9) gives the relation between the radius and the time. The final result is:

$$V_{w,i}' = \Psi \cdot \int_{\approx 10}^{t_i^{1/3}} f(t) \cdot t^{1/3} \cdot dt \tag{4.18}$$

Where the constant Ψ is:

$$\Psi = \frac{1}{3^{1/3} \cdot (4\pi)^{2/3}} \cdot [q'/\rho_o]^{5/3} = 0{,}128 \cdot [q'/\rho_o]^{5/3} \qquad (4.19)$$

The function f(t) is the radius distribution function in which r has been substituted by t using the relation Eq (4.9).

It is the effective degree of saturation and not the real degree of saturation that should be used for calculating the residual airpore spacing; see eq (1.2a).

By utilizing eq (4.10) to (4.12) one can calculate the process of air transport from the airpore system and consequently the time process of water-filling of the airpore system.

A simplification made in the derivation is that the the density of air is supposed to be constant. In reality, the density increases as the bubble decreases in size; see eq (3.4). This means that the calculated water absorption is a bit too high. On the other hand, the cross section of diffusion is assumed to decrease in proportion to the decrease in bubble size; see eq (3.31). In reality, the cross section is almost constant and determined by the radius of the pore itself. This leads to a too high clculated rate of air diffusion. The two effects compensate each other fairly well.

4.2.2 Numerical example 1; exponential function of pore radius

The pore size distribution can be determined by means of microscopical examinations (e.g. ASTM C457) or by automatic image analyses of thin sections or polished impregnated surfaces. The observed one- or two-dimensional pore data are transformed into a three-dimensional pore radius distribution using conventional stereomeric laws. From them the specific surface and the pore volume can be calculated.

A mathematical frequency function that sometimes fit an airpore distribution in a fair manner is:

$$f(r) = a_1 \cdot \frac{\ln b}{b^r} \qquad (4.20)$$

Where b is a constant that expresses the shape of the distribution and a_1 is a constant that is determined by the condition that the total pore volume calculated by eq (4.21) shall be equal to the real pore volume. The larger the value of b the smaller the average pore size and the more narrow the frequency function. The frequency function is shown in Fig 4.3 for different values of b. The curves are normalized to the same total airpore volume; i.e. the coefficient a is adjusted so that all distributions give the same total volume as the distribution

with b=1,051. The corresponding pore size distributions are plotted in Fig 4.4: The air pore volume is (for a_1=1); c.f. eq (1.4):

$$V_a' = \int_0^\infty \frac{\ln b}{b^r} \cdot \frac{4\pi}{3} \cdot r^3 \cdot dr = \frac{8\pi}{(\ln b)^3} \quad [m^3] \qquad (4.21)$$

As the lower integration limit 0 μm is used and not 10 μm as it should be according to the reasoning above. This makes the integration easier. Since the pore volume in pores smaller than 10 μm is very low, the error is negligible.

The real airpore volume is V_a. It can be obtained by the microscopical analysis mentioned above. Thus, by comparing V_a' from eq (4.21) with the measured V_a, the real distribution F(r) can be calculated; eq (4.3).

The calculated total envelope area A_a' of all pores is; c.f. eq (1.5):

$$A_a' = \int_0^\infty \frac{\ln b}{b^r} \cdot 4\pi \cdot r^2 \cdot dr = \frac{8\pi}{(\ln b)^2} \quad [m^2] \qquad (4.22)$$

Thus, the specific surface α_o of the airpore system is:

$$\alpha_o = V_a'/A_a' = \ln b \quad [m^2/m^3 = m^{-1}] \qquad (4.23)$$

Or:

$$b = \exp(\alpha_o) \qquad (4.24)$$

Thus, the coefficient b can be obtained from the experimentally determined specific surface. The value of b depends on the unit selected for volume and surface. The most convenient is to use μm. The following values are valid for a_1=1(the units for V_a' and A_a' are μm^3 and μm^2 respectively):

* α_o=60 mm^{-1} ≡0,06 μm^{-1}; b=1,062; $V_a' = 1{,}16 \cdot 10^5$; $A_a' = 6{,}94 \cdot 10^3$
* α_o=50 mm^{-1} ≡0,05 μm^{-1}; b=1,051; $V_a' = 2{,}04 \cdot 10^5$; $A_a' = 1{,}02 \cdot 10^4$
* α_o=40 mm^{-1} ≡0,04 μm^{-1}; b=1,041; $V_a' = 3{,}87 \cdot 10^5$; $A_a' = 1{,}56 \cdot 10^4$
* α_o=30 mm^{-1} ≡0,04 μm^{-1}; b=1,031; $V_a' = 8{,}83 \cdot 10^5$; $A_a' = 2{,}70 \cdot 10^4$
* α_o=20 mm^{-1} ≡0,02 μm^{-1}; b=1,020; $V_a' = 3{,}24 \cdot 10^6$; $A_a' = 6{,}41 \cdot 10^4$
* α_o=10 mm^{-1} ≡0,01 μm^{-1}; b=1,010; $V_a' = 2{,}55 \cdot 10^7$; $A_a' = 2{,}54 \cdot 10^5$

From the specific surface as it is defined above a sort of mean pore radius r_{mean} of the entire pore system can be calculated:

$$r_{mean} = 3/\alpha_o \qquad (4.25)$$

Or, for the actual distribution:

$$r_{mean} = 3/\ln b \qquad (4.26)$$

This is not the same as the radius of the median pore. This is defined:

$$r_{median} = \frac{\int_{\approx 10\mu m}^{\infty} r \cdot f(r) \cdot dr}{\int_{\approx 10\mu m}^{\infty} f(r) \cdot dr} \qquad (4.27)$$

For the actual frequency function the solution of this equation is:

$$r_{median} = \frac{\int_{o}^{\infty} r . \frac{\ln b}{b^r} . dr}{\int_{o}^{\infty} \frac{\ln b}{b^r} . dr} = \frac{4\pi}{3 \cdot \ln b} \qquad (4.28)$$

The relation in size between the two types of average pore is:

$$r_{median}/r_{mean} = 4\pi/9 = 1,40$$

The actual values of those radii are:

α_o=50 mm^{-1}:	r_{mean}= 60 μ m	r_{median}= 84 μ m
40	75	105
30	100	140
20	150	210
10	300	420

Model 1 has been applied to some distributions of this type. The results of the calculations are listed in APPENDIX 1. In Fig 4.5 the relation between the parameter $t \cdot q'/\rho_o$ and the **real degree of saturation** is plotted in log-log scale. The relations are non-linear seen over the entire span of degree of saturation. For the most interesting interval $0,1<S_a(t)<0,6$ the relations are, however fairly linear. Then, the following equation can be used:

$$S_a(t) = A\cdot[(t\cdot q')/\rho_o']^B \qquad 0,1<S_a(t)<0,6 \qquad (4.29)$$

Where A and B are constants which are obtained by linear regression in the log-log scale. Values of the two coefficients are listed in Table 4.1. The parameter inside the parenthesis must have the unit μm^3 when the values in Table 4.1 are used. Hence, the density of air ρ_o' must be expressed in $kg/\mu m^3$ i.e $\rho_o' = 1,25\cdot10^{-18}\ kg/\mu m^3$ at +10 °C.

Table 4.1: The coefficients A and B in Eq (4.29)

Specific surface μm^{-1}	b	A	B
0,050	1,051	$23,48\cdot10^{-5}$	0,575
0,040	1,041	$12,55\cdot10^{-5}$	0,593
0,030	1,031	$7,36\cdot10^{-5}$	0,597
0,020	1,020	$4,30\cdot10^{-5}$	0,583
0,010	1,010	$1,15\cdot10^{-5}$	0,589

A general equation is:

$$\mathbf{S_a(t) = 3,27\cdot10^{-8}\cdot\alpha_o^{2,27}\cdot[(t\cdot q')/\rho_o']^{0,587}} \qquad (4.30)$$

Where α_o is expressed in mm^{-1}.

According to this equation the long term absorption in airpore systems is approximately proportional to the square-root of time.

The coefficient q′ expressing the rate of air diffusion can be calculated by eq (3.33). The following data are used: (i) the diffusivity δ is either $10^{-11}\ m^2/s$ or $10^{-12}\ m^2/s$; (ii) the solubility of air s is $2,5\cdot10^{-7}\ kg/(m^3\cdot Pa)$; (iii) the relation ε between the average transport distance of air and the bubble radius is 5; (iv) the surface tension σ is 0,074 N/m.Then the diffusion rate q′is $5,6\cdot10^{-18}$kg/s. Eq (4.30) can be written:

$$S_a(t) = 7,9\cdot10^{-8}\cdot\alpha_o^{2,27}\cdot t^{0,587} \qquad (\delta = 10^{-11}\ m^2/s) \qquad (4.31a)$$

$$S_a(t) = 2,0\cdot10^{-8}\cdot\alpha_o^{2,27}\cdot t^{0,587} \qquad (\delta = 10^{-12}\ m^2/s) \qquad (4.31b)$$

Where t is in seconds and α_o is expressed in mm^{-1}. These equations have been plotted in Fig 4.6. The rate of absorption is rather rapid which is mainly due to the rather high value 0,587 of the exponent. It might also depend, to some extent, on the values chosen for the diffusivity. They might be too large.

The real size distribution can in some cases be better described by a sum of two distributions of type eq (4.20).

$$f(r) = C \cdot \frac{\ln b_1}{b_1^r} + D \cdot \frac{\ln b_2}{b_2^r} \qquad (4.32)$$

Where the constants C and D are selected in such a way that the total airpore distribution f(r) corresponds to the real distribution.

Then the solutions tabulated in APPENDIX 1 for the individual distributions can be used.

Example 4.1: An airpore distribution is composed of one distribution of type 1 with b=1,031 and another distribution of type 2 with b=1,020. Half the pore volume belongs to distribution 1 and the other half to distribution 2. This means that the ratio of the constants $C/D = 3{,}24 \cdot 10^6 / 8{,}83 \cdot 10^5 = 3{,}67$; see the list above of V_a'-values for different b-values.

The specific surface of the combined distribution is:

$$\alpha_o = \frac{3{,}67 \cdot 2{,}70 \cdot 10^4 + 1 \cdot 6{,}41 \cdot 10^4}{3{,}67 \cdot 8{,}83 \cdot 10^5 + 1 \cdot 3{,}24 \cdot 10^6} = 0{,}025\ \mu m^{-1} \equiv 25\ mm^{-1}$$

The S_a-value after a certain time of water absorption in the airpore system is the mean of the two S_a-values for the two distributions. These are listed in APPENDIX 1.

The resulting relation between the degree of saturation in the airpore system, S_a, and the suction time is plotted in Fig 4.5. The general shape of the curve for the combined distribution is the same as for the single distributions; i.e. the exponent in eq (4.30) is about the same; 0,525 instead of the value 0,587.

The fact that the calculated water absorption is rapid for the type of airpore distribution treated in this chapter might, however also depend on the model itself implying that a larger bubble can start to absorb water before the smaller bubbles are filled. Below, in section 4.3 it is shown that Model 2 gives a considerably slower absorption.

The effective degree of saturation defined by eq (4.16) can be calculated analytically utilizing Eq(4.18) and (4.19). The following relation for the volume of completely water-filled pores is valid for the actual type of distribution:

$$V_{w,i}' = \Psi \cdot \int_{\approx 10}^{t_i^{1/3}} \frac{\ln b}{[3 \cdot q'/(4\pi \cdot \rho_o)]^{1/3}} \cdot \frac{t^{1/3}}{b} \cdot dt \qquad (4.33)$$

Where the constant Ψ is given by Eq (4.19). This equation can be solved analytically giving the relation between suction time and degree of saturation.

The effective degree of saturation is obtained by dividing the values $V_{w,i}'$ by the total airpore volume V_a'. Calculated values are listed in APPENDIX 2. The relation between the real and the effective degrees of saturation are plotted in Fig 4.7. The relation is almost linear in a log-log scale and independent of the specific surface of the pore system. The following relation is valid:

$$S_{a,eff} = 0{,}918 \cdot S_a^{1{,}45} \qquad (4.34)$$

This means that a considerable fraction of the absorbed water is contained in pores that are coarser than the colmpletely water-filled finer pores.

Example 4.2: The effective degree of saturation is only 0,34 when the real degree of saturation is 0,50. This means that only 68 % of the water is contained in completely water-filled pores and the rest in coarse, partly air-filled pores.

4.2.3 Numerical example 2; power function of pore radii

An alternative frequency function of pore radii is:

$$f(r) = a_2 \cdot \{\frac{1}{r^b} - \frac{1}{r_{max}^b}\} \qquad (4.35)$$

Where a_2 is a constant which is determined by the total airpore volume. b is a constant that gives the shape of the distribution. r_{max} is the radius of the largest pore. The frequency function is plotted in Fig 4.3 together with the exponential frequency function. The coefficient a_2 is adjusted so that the same total pore volume is obtained as for the other frequency curves. The power function gives a much more broad distribution than does the exponential function. The pore volume distribution curve is shown in Fig 4.8. The pore volume is much more concentrated to the coarser pores than what is the case with

the exponential function; c.f Fig 4.3.

The total airpore volume is (for $a_2=1$):

$$V_a' = \frac{\pi}{3} \cdot \frac{b}{4-b} \cdot \{r_{max}^{4-b} - r_{min}^{4-b}\} \qquad (4.36)$$

The total surface area is:

$$A_a' = \frac{4\pi}{3} \cdot \frac{b}{3-b} \{r_{max}^{3-b} - r_{min}^{3-b}\} \qquad (4.37)$$

The specific surface is:

$$\alpha_o = 4 \cdot \frac{4-b}{3-b} \cdot \frac{r_{max}^{3-b} - r_{min}^{3-b}}{r_{max}^{4-b} - r_{min}^{4-b}} \qquad (4.38)$$

A resonable value of r_{min} and r_{max} are 10 µm and 1000 µm. Then, the following values are valid. (The units for V_a' and A_a' is µ m^3 and μm^2):

* $\alpha_o=50\ mm^{-1} \equiv 0,05\ \mu m^{-1}$ b=3,65 $V_a'=98,0$ $A_a'=5,0$
* $\alpha_o=30\ mm^{-1} \equiv 0,03\ \mu m^{-1}$ b=3,30 $V_a'=596,5$ $A_a'=17,3$
* $\alpha_o=10\ mm^{-1} \equiv 0,01\ \mu m^{-1}$ b=2,50 $V_a'=55100$ $A_a'=595,8$

The median pore radius is:

$$r_{median} = 0,5 \cdot \frac{1-b}{2-b} \cdot \frac{r_{max}^{2-b} - r_{min}^{2-b}}{r_{max}^{1-b} - r_{min}^{1-b}} \qquad (4.39)$$

The following values are valid:

$\alpha_o=50\ mm^{-1}$	$r_{median}=$ 8,0 µm	$r_{mean}=$ 60 µm	$r_{med}/r_{mean}=$ 0,13
30	8,8	75	0,12
10	13,5	300	0,045

The median pore is much smaller than the mean pore defined by the specific surface. This is explained by the large number of pores in the very small size range. They provide a large surface area without containing much pore volume.

Some results of a calculation of the real and effective degrees of saturation versus the suction time are listed in APPENDIX 3.

In Fig 4.9 the real degree of saturation is plotted versus the

parameter $t \cdot q'/\rho_o$. The relation is fairly linear in a log-log scale. Therefore, the same type of relation as Eq (4.29) can be used:

$$S_a(t) = A' \cdot [(t \cdot q'/\rho_o)]^{B'} \quad 0,1 < S_a(t) < 0,6 \qquad (4.40)$$

The coefficients A´ and B´ are listed in Table 4.2. Note: ρ_o in Eq (4.40) must be expressed in $kg/\mu m^3$.

Table 4.2: The coefficients A´and B´in Eq (4.40).

Specific surface mm^{-1}	A´	B´
50	$1,47 \cdot 10^{-2}$	0,208
30	$2,89 \cdot 10^{-3}$	0,280
10	$4,84 \cdot 10^{-5}$	0,465

A general equation is:

$$S_a(t) = 1,33 \cdot 10^{-8} \cdot \alpha_o^{3,58} \cdot [t \cdot q'/\rho_o)]^{1,46 \cdot \alpha_o^{-0,49}} \qquad (4.41)$$

Where α_o is expressed in mm^{-1}.

In Fig 4.10 the real degree of saturation is plotted versus the suction time for two diffusivities; $\delta = 10^{-11}$ m^2/s and $\delta = 10^{-12}$ m^2/s. The power function distribution evidently gives a considerably slower water absorption than does the exponential distribution.

Example 4.3: Two concretes with different types of the airpore system are compared. The specific surface of the pore system is the same, 30 mm^{-1}. This means that the mean value of the pore radius is the same (100 μm) but the median pore radius and the shape of the volume size distribution is different; see above. The diffusivity of air diffusion is $\delta = 10^{-11}$ m^2/s. The time needed to reach a real degree of saturation of 0,5 is calculated.

* Exponential function: Eq (4.31a) gives: $t = 7,5 \cdot 10^5$ sec ≡ **9 days** for $S_a = 0,5$.

* Power function: Eq (4.41) gives: $t = 2,2 \cdot 10^7$ sec ≡ **260 days** for $S_a = 0,5$.

The effect of the fineness of the pore system is very large in both models:

Example 4.4: The same as example 4.3 but the specific surface is only 10 mm^{-1}.

* Exponential function: Eq (4.31a) gives: $t = 5{,}2 \cdot 10^7$ sec ≡ **600 days ≡ 1,6 years** for $S_a = 0{,}5$.

* Power function: Eq (4.41) gives: $t = 10^8$ sec ≡ **1160 days ≡ 3,2 years** for $S_a = 0{,}5$.

The analysis therefore shows that the shape of the airpore system has a very large effect on the rate by which the airpore system becomes water-filled.

The effective degree of saturation is almost directly proportional to the real degree of saturation. The proportionality coefficient is somewhat dependent of the pore size distribution; see Fig 4.11.

4.3 Model 2: Absorption in consecutive order of pore size

4.3.1 Theory

The model is described graphically in Fig 4.2. A larger pore does not start to absorb water until a smaller pore is completely water-filled. Therefore, the total amount of air transferred after a certain time t_i which corresponds to the time when the pores with radius r_i finally become completely water-filled is:

$$V'_i = \int_{\approx 10\mu m}^{r_i} \rho_o \cdot \frac{4\pi}{3} \cdot r^3 \cdot f(r) \cdot dr \approx \sum_{1}^{i} \rho_o \cdot V'(r_{m,i}) \qquad (4.42)$$

Where $V'(r_{m,i})$ is the total volume of all pores with radii between r_i and r_{i+1}; see Eq (4.8).

The time t_i is:

$$t_i = \sum_{j}^{i} t(r_{m,j}) \qquad (4.43)$$

Where $t(r_{m,j})$ is defined by Eq (4.9). It is the time needed to

fill a bubble with the initial radius $r_{m,j}$. Thus, the solutions for the effective degree of saturation of the pore system tabulated in APPENDICI 1-2 for different airpore distributions can be used if the time columns in the appendici are changed. The suction time corresponding to a certain effective degree of saturation is the sum of all times in the time column for all the pores smaller than and equal to the actual pore corresponding to the actual degree of saturation. In Model 2, the real and the effective degrees of saturation coincide since no water is assumed to be contained in pores that are bigger than the biggest completely water-filled pore.

4.3.2 Numerical example 1; exponential function of pore radius

The frequency function is given in Eq (4.20). The degree of saturation versus the parameter $t \cdot q'/\rho_o$ is plotted in Fig 4.12 in log-log scale. The curves are non-linear. However, in the span $0,1<S_{a,eff}<0,6$ an approximative relation can be used:

$$S_a(t)_{eff} = A'' \cdot [(t \cdot q'/\rho_o)]^{B''} \qquad 0,1<S_a(t)_{eff}<0,6 \qquad (4.44)$$

Where A'' and B'' are constants obtained by linear regression in the log-log scale. The values are listed in Table 4.3. Note: The unit of the parameter $t \cdot q'/\rho_o$ is μm^3.

Table 4.3: The coefficients A'' and B'' in Eq (4.44)

Specific surface μm^{-1}	b	A''	B''
0,050	1,051	$2,87 \cdot 10^{-4}$	0,500
0,040	1,041	$1,98 \cdot 10^{-4}$	0,497
0,030	1,031	$7,48 \cdot 10^{-5}$	0,523
0,020	1,020	$3,61 \cdot 10^{-5}$	0,535
0,010	1,010	$2,75 \cdot 10^{-7}$	0,722

A general equation for specific surfaces in the range $20<\alpha_o<50$ mm^{-1} is:

$$\mathbf{S_a(t)_{eff} = S_a = 2,93 \cdot 10^{-8} \cdot \alpha_o^{2,36} \cdot [t \cdot q'/\rho_o]^{0,51}} \qquad \mathbf{(4.45)}$$

Where α_o is expressed in mm^{-1}.

The degree of saturation as function of the suction time is plotted in Fig 4.13 for the two diffusivities $\delta = 10^{-11}$ m^2/s and $\delta = 10^{-12}$ m^2/s. Then eq (4.45) is written:

$$S_a(t)_{eff} = 6{,}30 \cdot 10^{-8} \cdot \alpha_o^{2{,}36} \cdot t^{0{,}51} \quad (\delta = 10^{-11}\ m^2/s) \qquad (4.46a)$$

$$S_a(t)_{eff} = 1{,}95 \cdot 10^{-8} \cdot \alpha_o^{2{,}36} \cdot t^{0{,}51} \quad (\delta = 10^{-12}\ m^2/s) \qquad (4.46b)$$

The degree of saturation is almost exactly proportional to the square-root of the suction time. The degree of saturation does therefore evolve considerably more slowly in Model 2 than in Model 1 where the exponent was 0,59. Besides, the time-scale is extended since a certain pore does not start to absorb water until all smaller pores are full.

Example 4.5: Consider a pore system with $\alpha_o = 30$ mm^{-1}. The diffusivity $\delta = 10^{-11}$ m^2/s. An analysis is made of the time to reach the degree of saturation $S_a = 0{,}5$ or $S_{a,eff} = 0{,}5$ in the airpore system.

Model 1: Eq (4.31a) gives: $t = 7{,}5 \cdot 10^5$ sec ≡ **9 days** for $S_a = 0{,}5$.

Eq (4.31a) gives: $t = 1{,}2 \cdot 10^6$ sec ≡ **14 days** for $S_{a,eff} = 0{,}5$ corresponding to $S_a = 0{,}66$ [Eq (4.34)].

Model 2: Eq (4.46a) gives: $t = 5{,}0 \cdot 10^6$ sec ≡ **58 days** for $S_a = S_{a,eff} = 0{,}5$.

For a dense material with rather coarse airpores Model 2 predicts that the degree of saturation is low even after a long time of continuous water suction; e.g. after 10 years, the effective degree of saturation is only about 0,2 to 0,5 when the specific surface is 10 mm^{-1} to 20 mm^{-1}.

4.3.3 Numerical example 2; power function of pore radius

The frequency function is given in Eq (4.35). The degree of saturation is listed in APPENDIX 3. It is plotted in Fig 4.14 versus the parameter $t \cdot q'/\rho_o$. The following relation can be used in the most interesting range of degree of saturation:

$$S_a = A''' \cdot [(t \cdot q')/\rho_o]^{B'''} \qquad (4.47)$$

The constants A''' and B''' are listed in Table 4.4.

Table 4.4: The coefficients A´´´and B´´´in Eq (4.47).

Specific surface mm^{-1}	A´´´	B´´´
50	$2,03 \cdot 10^{-2}$	0,171
30	$5,75 \cdot 10^{-3}$	0,224
10	$1,52 \cdot 10^{-5}$	0,477

A general equation is:

$$S_a(t)_{eff} = S_a = 4,47 \cdot 10^{-10} \cdot \alpha_o^{4,49} \cdot [t \cdot q' / \rho_o]^{2,08 \cdot \alpha_o^{-0,65}} \qquad (4.48)$$

Where α_o is in mm^{-1}.

The degree of saturation as function of the suction time is plotted in Fig 4.15 for the two diffusivities $\delta = 10^{-11}$ m^2/s and $\delta = 10^{-12}$ m^2/s.

Model 2 gives a much slower water absorption. This is shown by the same example as 4.5 above but this time applied to the power function.

Example 4.6: Consider a pore system with α_o=30 mm^{-1}. The diffusivity is $\delta = 10^{-11}$ m^2/s. The time needed to reach a real or effective degree of saturation of 0,5 is analyzed.

Model 1: Table 4.2 gives: $t = 2,2 \cdot 10^6$sec ≡ **200 days** for S_a=0.5

$S_{a,eff}$ = 0,5 corresponds to S_a= 0,60 [Fig 4.11]. Then, Table 4.2 gives: $t = 4,2 \cdot 10^7$sec ≡ **490 days ≡ 1,3 years.**

Model 2: Table 4.4 gives: $t = 1,0 \cdot 10^8$sec ≡ **1160 days ≡ 3,2 years.**

Model 2 applied to a coarse-porous system gives a very slow water absorption.

Example 4.7: Consider a pore system with α_o=10 mm^{-1}. The diffusivity $\delta = 10^{-11}$ m^2/s. The time needed to fill the airpore system to a degree of saturation of 0,5 is:
$t=6,6 \cdot 10^8$ sec ≡ **7600 days ≡ 20 years.**
The time needed to fill it to 70% is $2 \cdot 10^9$sec ≡ **65 years.**

4.4 Concluding remarks

The time process of water absorption in the airpore system can be described by an equation of the following type:

$$S_a(t) = f(\delta) \cdot f(\text{pore shape}) \qquad (4.49)$$

The function $f(\delta)$ should principally be independent of the pore shape and the suction time. Often it has the following general appearance:

$$f(\delta) = c \cdot \delta^d \quad (d<1) \qquad (4.50)$$

Where c and d are constants. In some cases, e.g. for the pore pore distribution of the power type, the regression analysis indicates that the function $f(\delta)$ is also a function of the pore shape.

The function f(pore shape) is independent of the diffusivity but is very much dependent of the pore size distribution. A typical equation is:

$$f(\text{pore shape}) = e \cdot \alpha_o^f \cdot t^g \quad (g<1) \qquad (4.51)$$

Where e ,f and g are constants that depend on the shape of the pore size distribution. t is the water absorption time.

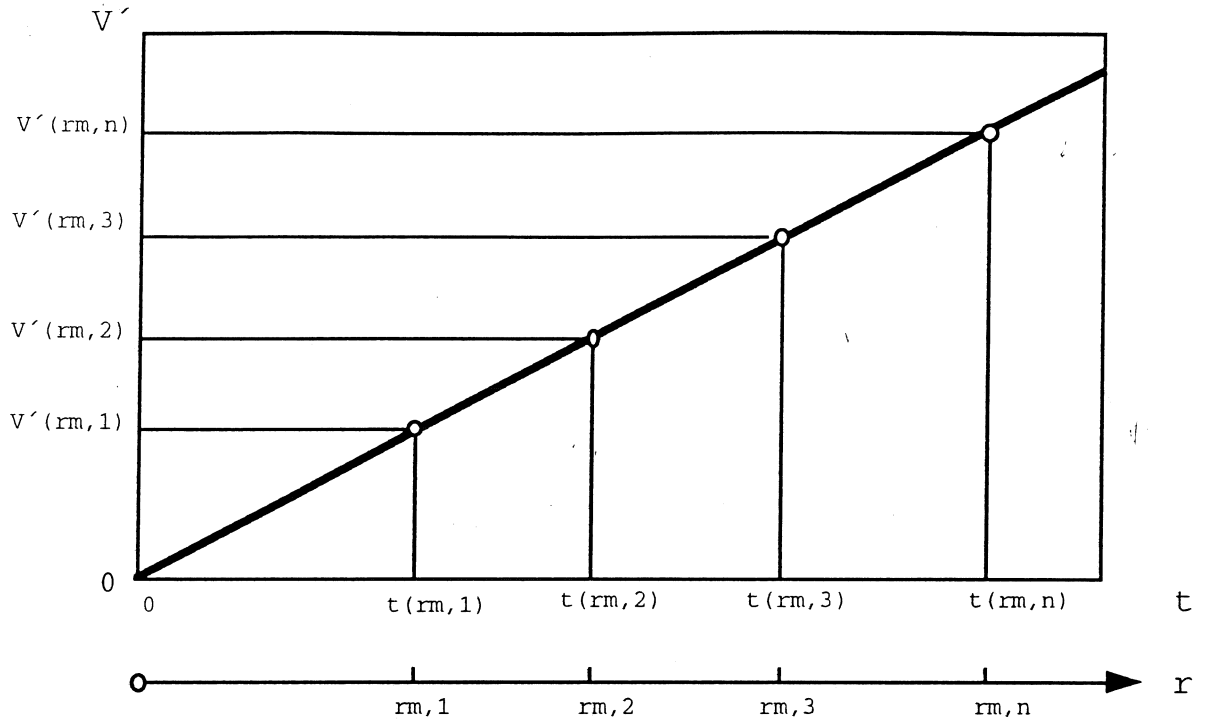

Fig 4.1: Graphical representation of Model 1 of water absorption in the airpore system.

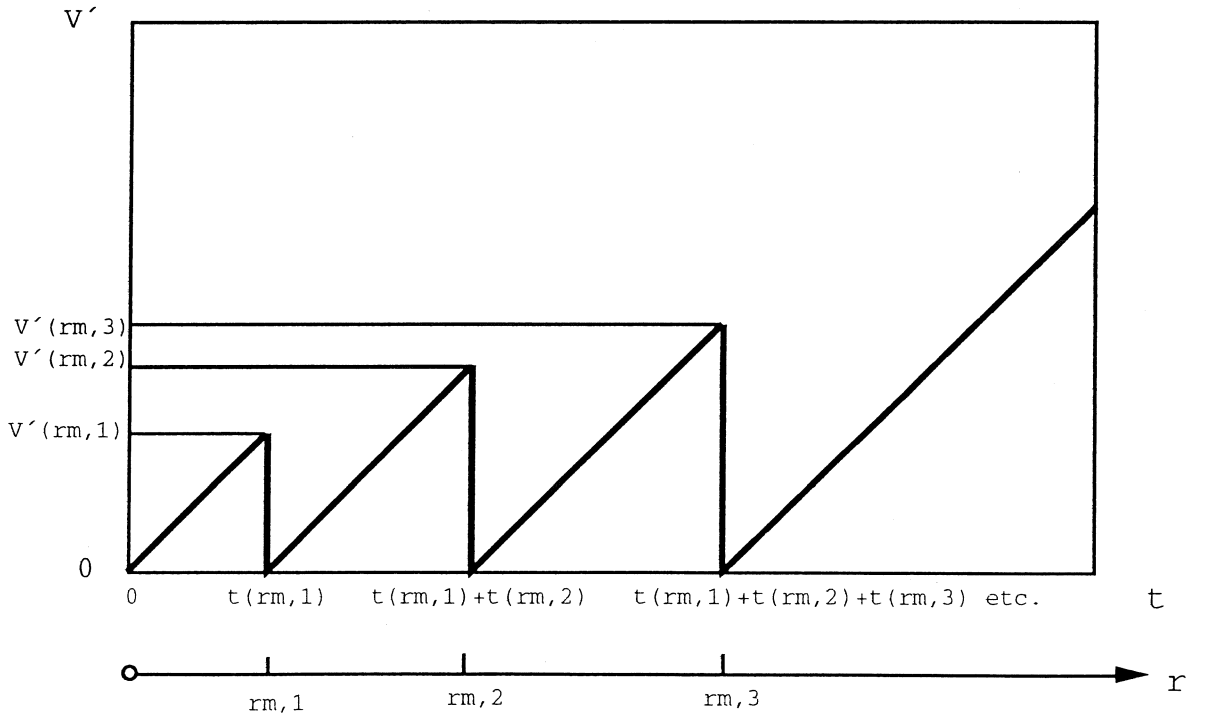

Fig 4.2: Graphical representation of Model 2 of water absorption in the airpore system.

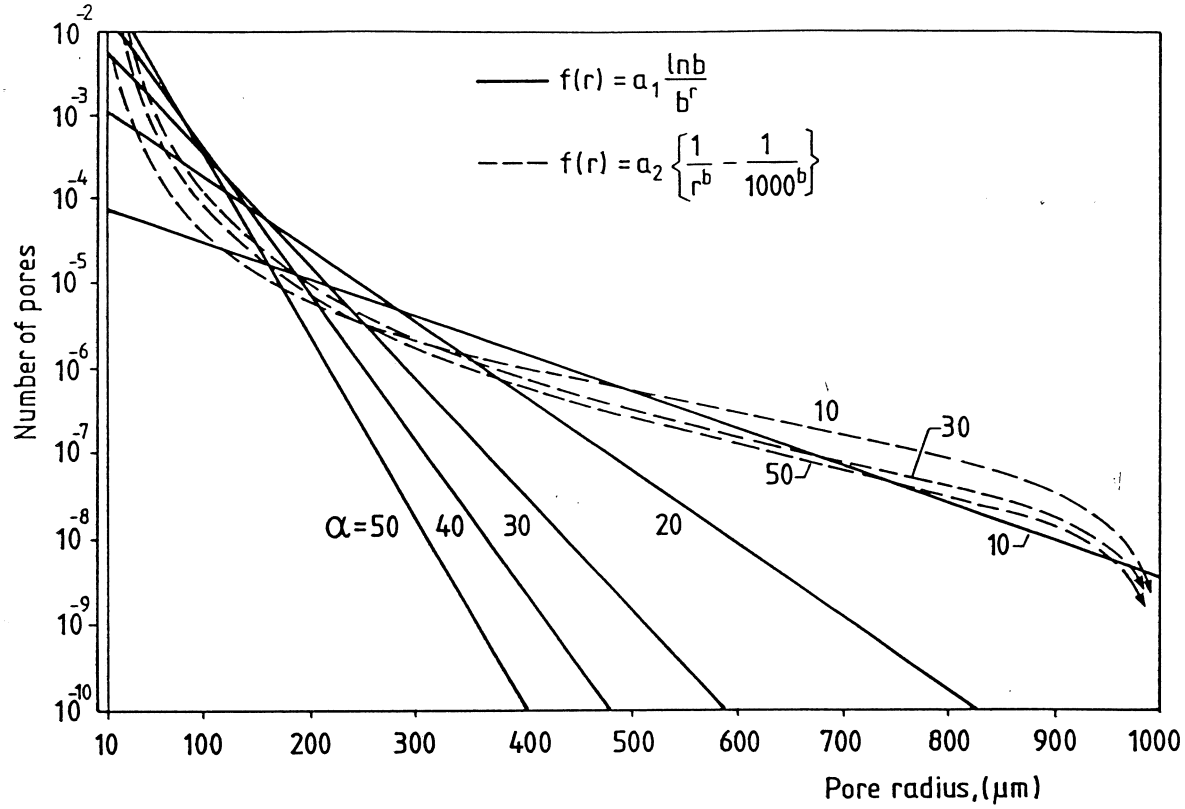

Fig 4.3: The frequency functions of the pore radius. Exponential function according to eq (4.20) and power function according to eq (4.35). The functions are normalized to equal total pore volume.

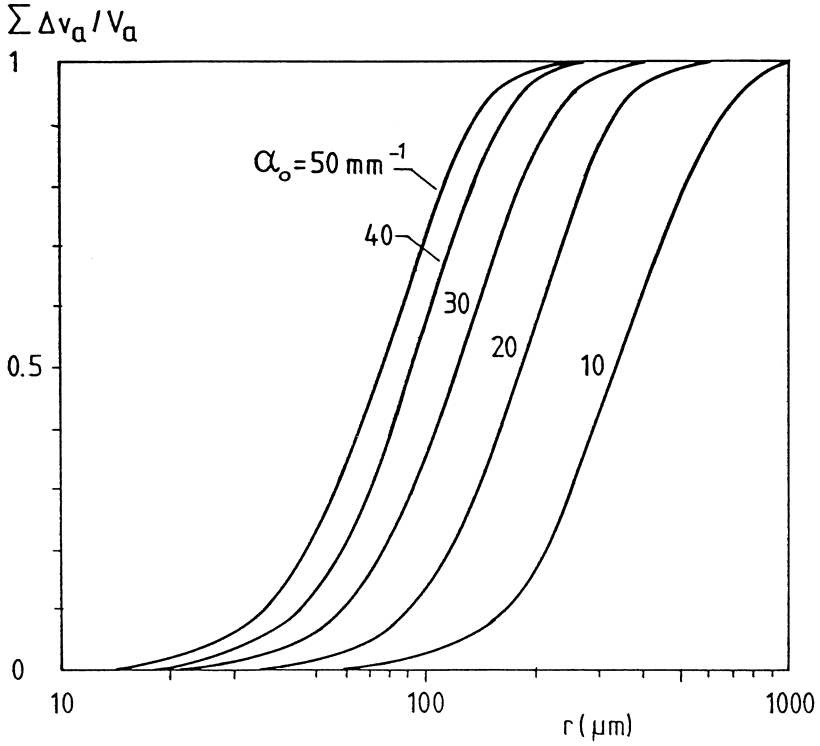

Fig 4.4: The pore size distribution according to the exponential frequency function in eq (4.20).

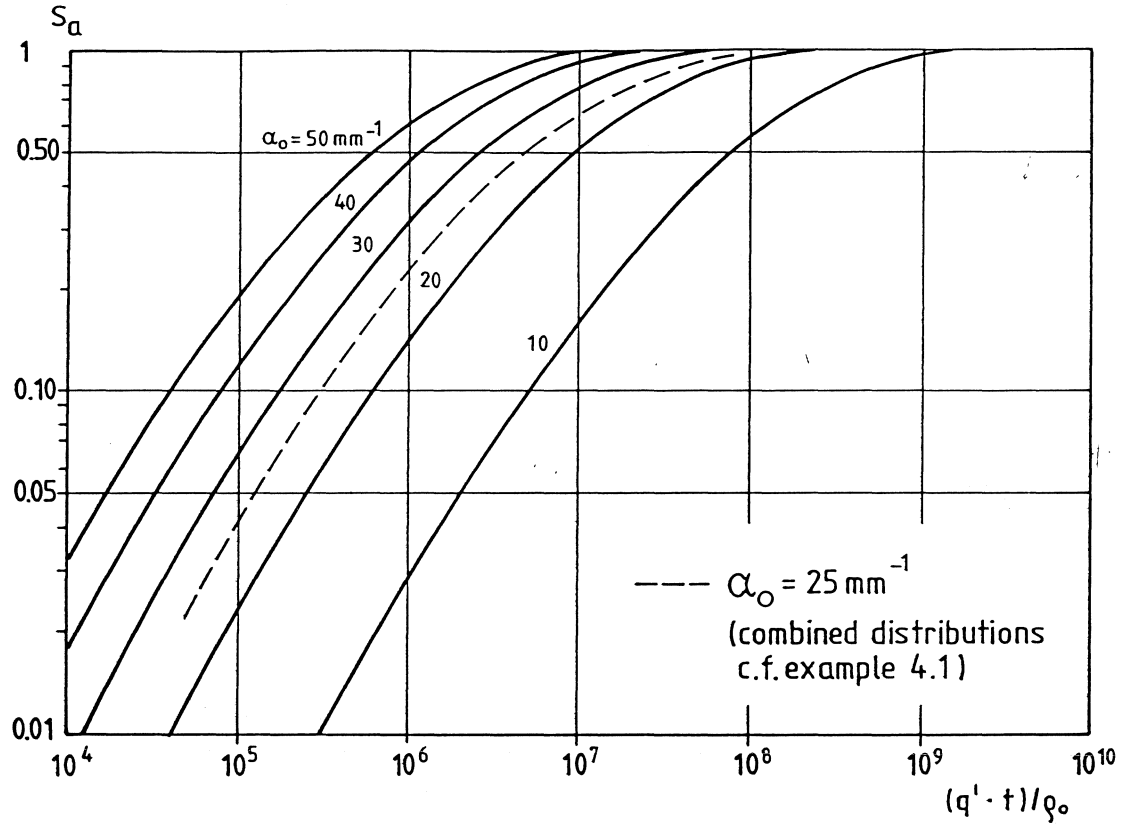

Fig 4.5: The real degree of saturation of the airpore system versus the water storage time expressed in terms of the parameter $t \cdot q'/\rho_o$. Exponential frequency function of pore radius. Absorption according to Model 1.

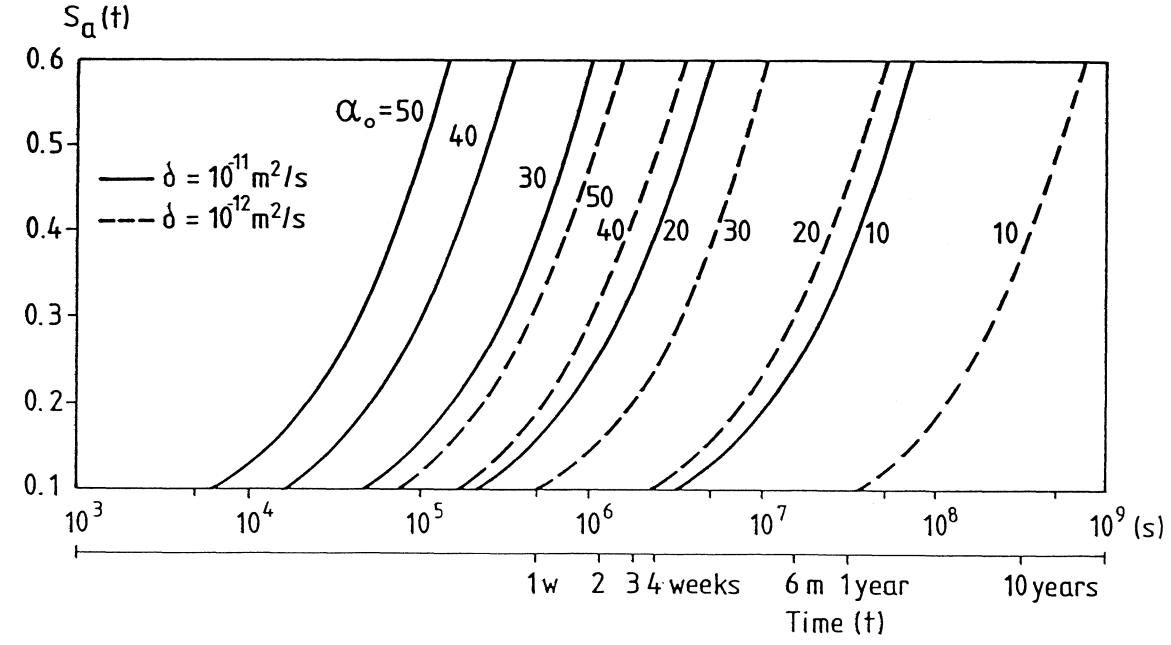

Fig 4.6: The real degree of saturation of the airpore system versus the water storage time for two different diffusivities of air transport through pore water. Exponential frequency function. Absorption according to Model 1.

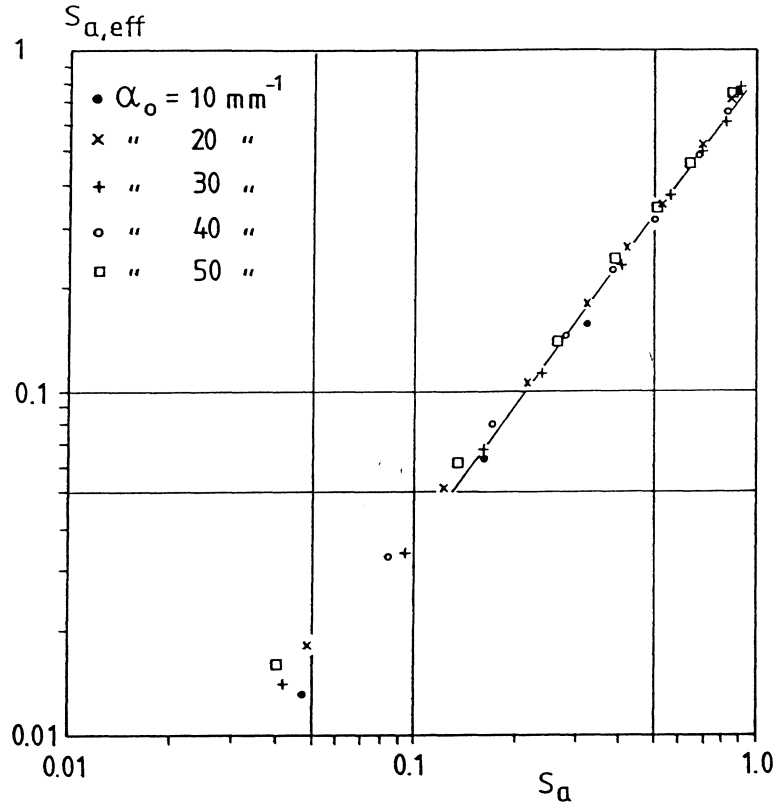

Fig 4.7: Relation between the real and the effective degrees of saturation of the airpore system. Exponential frequency function. Absorption according to Model 1.

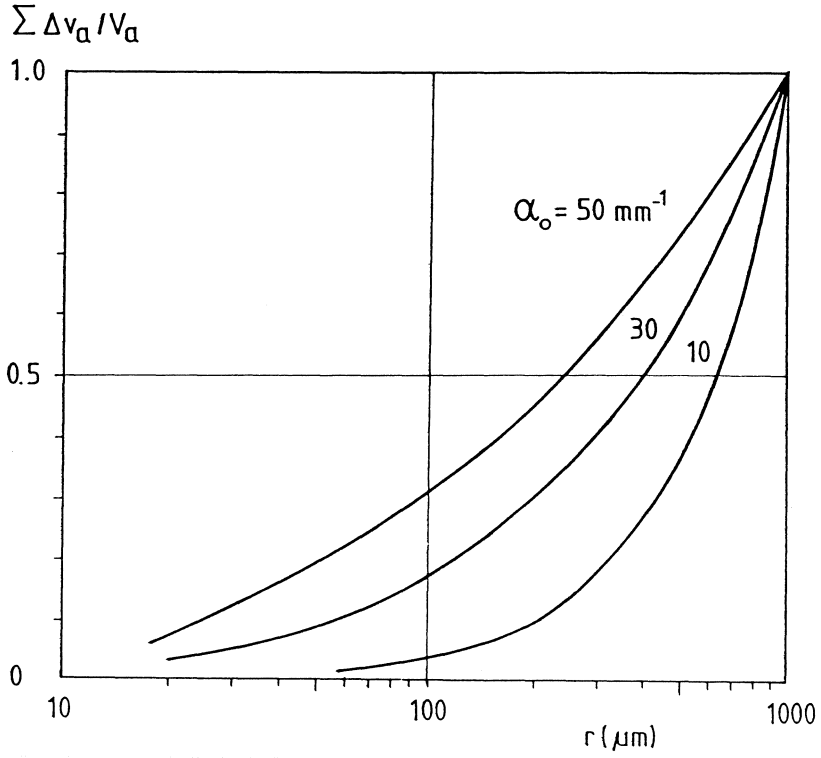

Fig 4.8: The pore size distribution according to the power frequency function in eq (4.35).

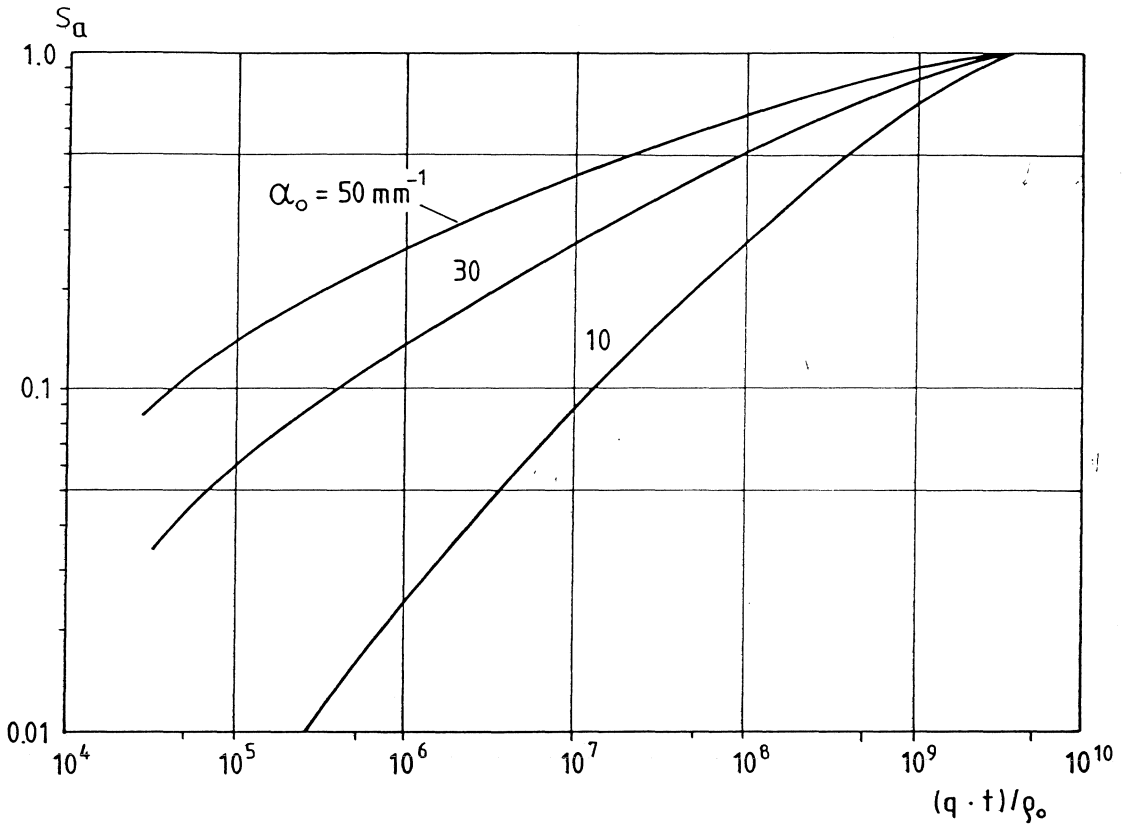

Fig 4.9: The real degree of saturation of the airpore system versus the water storage time expressed in terms of the parameter $t \cdot q'/\rho_o$. Power function of pore radius. Absorption according to Model 1.

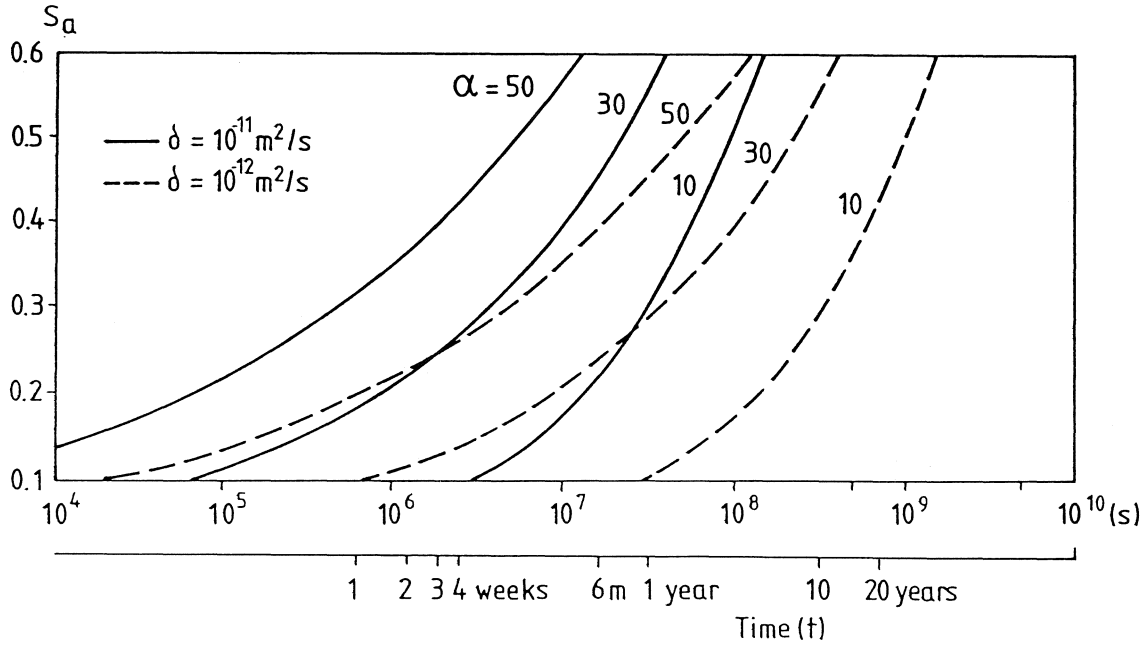

Fig 4.10: The real degree of saturation of the airpore system versus the water storage time for two different diffusivities of air transport through pore water. Power frequency function. Absorption according to Model 1.

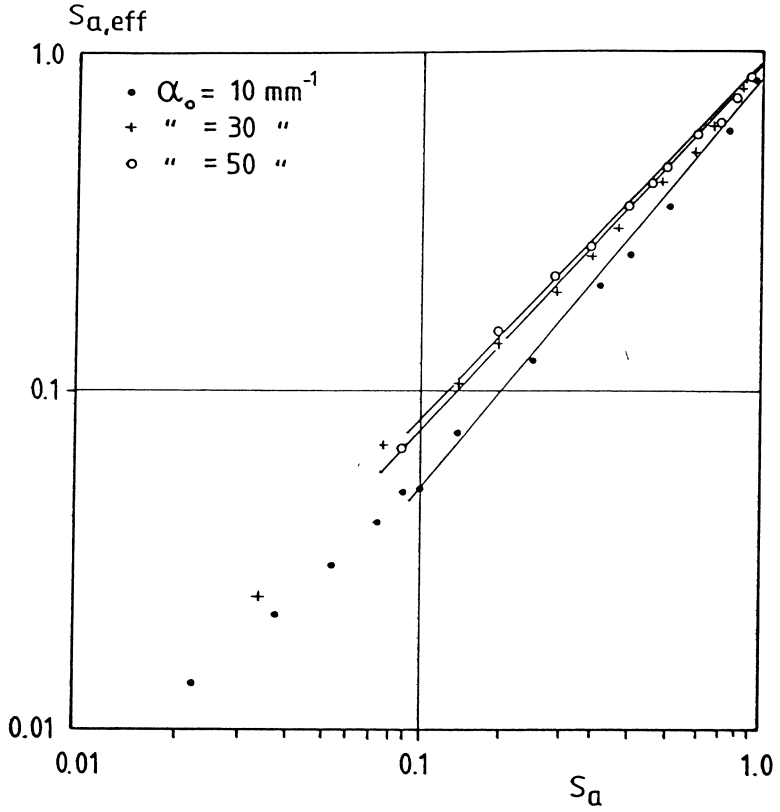

Fig 4.11: Relation between the real and the effective degrees of saturation of the airpore system. Power frequency function. Absorption according to Model 1.

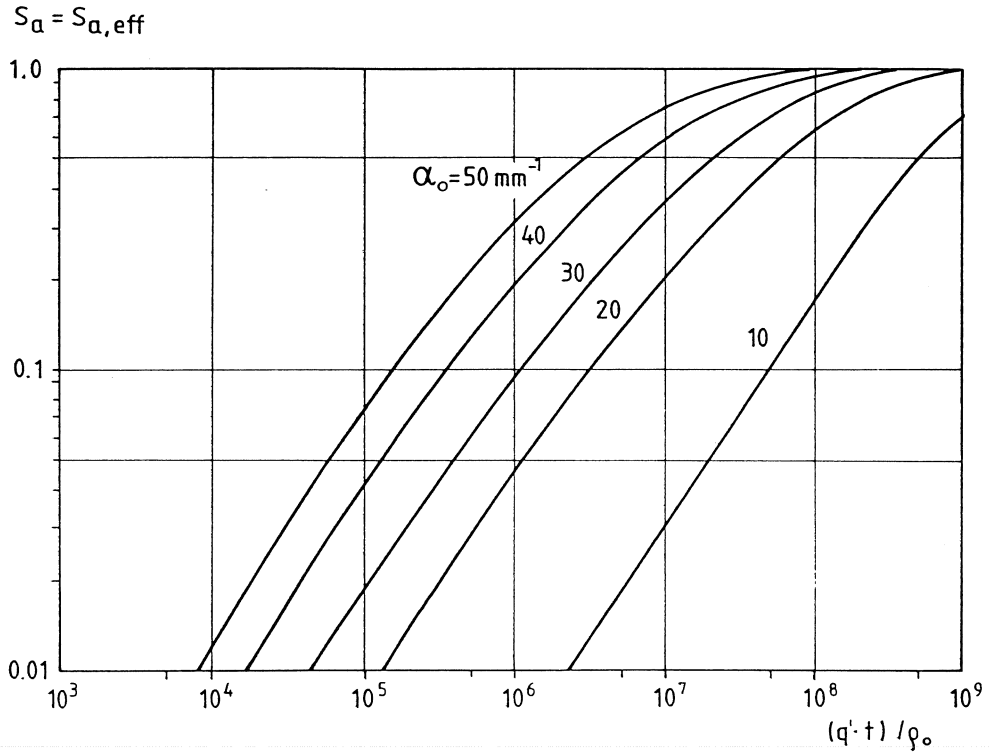

Fig 4.12: The real degree of saturation of the airpore system versus the water storage time expressed in terms of the parameter $t \cdot q' / \rho_o$. Exponential frequency function of pore radius. Absorption according to Model 2.

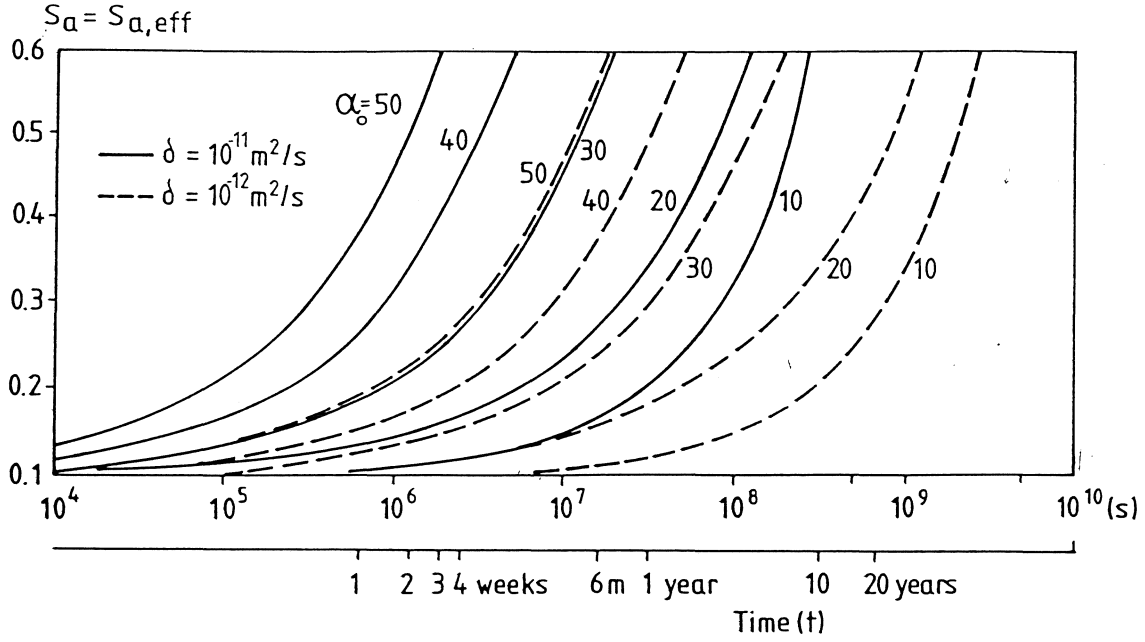

Fig 4.13: The real degree of saturation of the airpore system versus the water storage time for two different diffusivities of air transport through pore water. Exponential frequency function. Absorption according to Model 2.

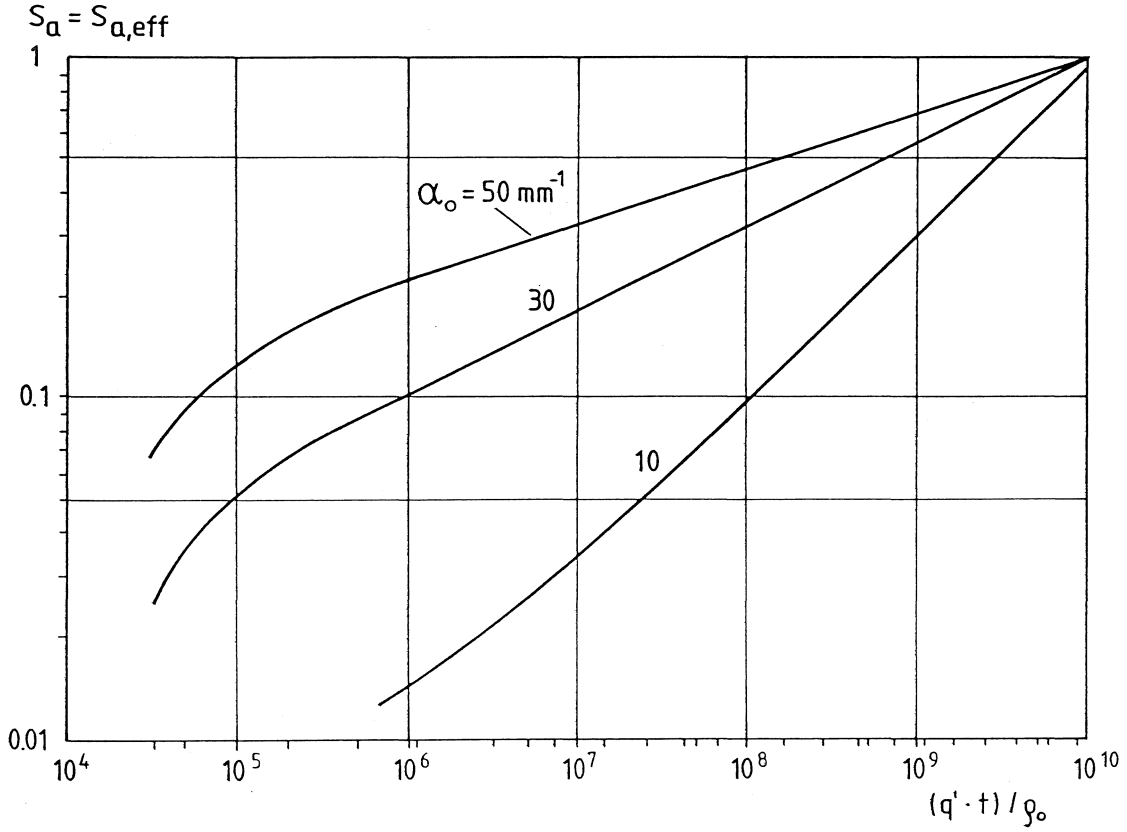

Fig 4.14: The real degree of saturation of the airpore system vesus the water storage time expressed in terms of the parameter $t \cdot q'/\rho_o$. Power frequency function of pore radius. Absorption according to Model 2.

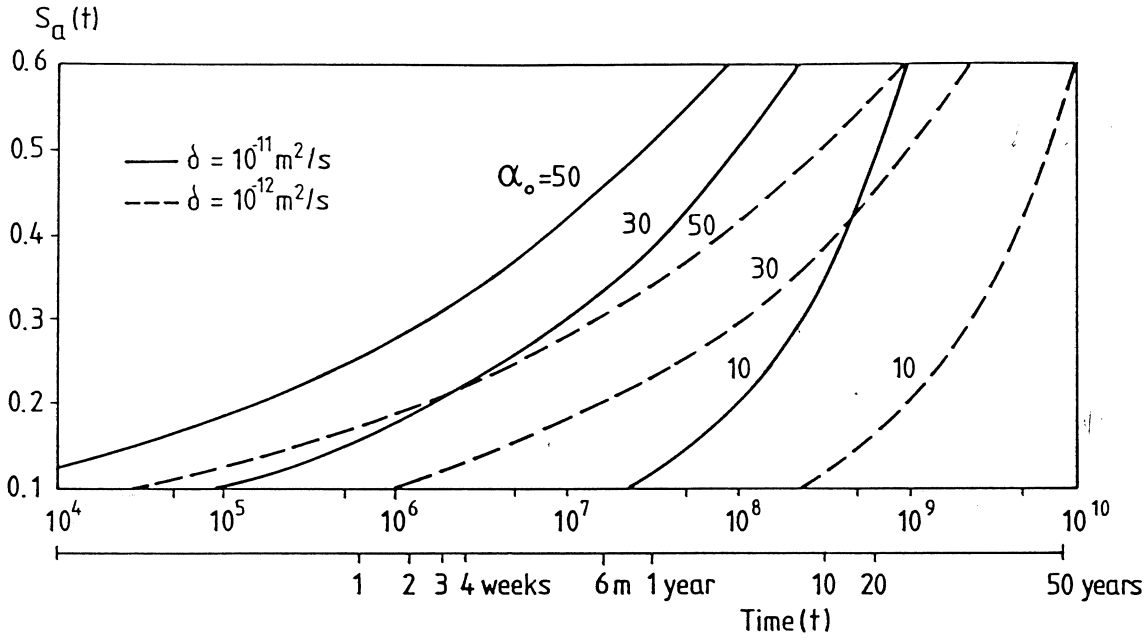

Fig 4.15: The real degree of saturation of the airpore system versus the water storage time for two diffusivities of air transport through pore water. Power frequency function of pore radius. Absorption according to Model 2.

5. Experimental results

5.1 Water absorption tests

The long term water absorption has been studied for a large number of concretes and cement mortars. The normal specimen type has been slices with a diameter of about 100 mm and a thickness of about 25 mm. The slices have been cut from concrete cylinders. In other tests cement mortars have been investigated. Then, the specimen is normally flat specimens with the height 15 to 20 mm, the width 40 to 50 mm and the length 120 to 160 mm.

In all cases, the specimens have been pre-dried in laboratory air and then placed on supports in a tray with water so that the water surface is about 1 mm above the bottom surface of the specimen. The weight increase of the specimens has been studied from the first 5 minutes of suction until the test was interrupted. The time interval between the individual measurements has been 5 to 10 minutes during the first hour, 1 hour during the first 8 hours, 24 hours during the first week and then about 1 week.The total test time has been different for different series. Normally it has been 14 days, 30 days or almost one year. During the whole time a watertight plexiglass lid has been placed on top of the tray in order to hinder evaporation from the top surface of the specimens.

It is appropriate to express the absorption in terms of the degree of saturation S of the entire pore system. A typical absorption-time curve looks like Fig 5.1. From the first rapid absorption during the first hour the capillary constants m, P_{cap}, k and q_c (see section 1.3) can be evaluated. The nick-point in the diagram corresponds to the instant when the water front reaches and wets the entire top surface. The slow water uptake after the nick-point is mainly due to the slow absorption in the airpore system. It is supposed to occur simultanously over the entire specimen volume if this is not too thick. Then, the nick-point absorption time t_n corresponds to time 0 in the airpore absorption process. A typical value of t_n is 10 hours for a specimen thickness of 20 to 25 mm. This time is so short in comparison with the time involved in the slow airpore absorption that an eventual error in it will be negligible.

The nick-point absorption S_n is calculated as the intersection between the two lines. These are obtained by linear regression at which the first steep line as supposed to be linear in a lin-square-root diagram whereas the second line during the first few days is linear in a lin-log diagram. The degree of saturation of the airpore system at time $(t-t_n)$ counted from the occurrence of the nick-point absorption is:

$$S_a(t-t_n) = \frac{S(t) - S_n}{1 - S_n} \qquad (5.1)$$

Where S(t) is the total degree of saturation of the concrete at time t counted from the start of the test.

An analysis of some of these tests will be presented below. The absorption in the airpore system will be expressed in terms of a power function of the following type which makes a direct comparison with the theoretical derivation in Section 4 possible:

$$S_a(t) = A \cdot t^B \qquad (5.2)$$

Where A and B are constants. The time t is in this case counted from the nick-point.

5.2 Tests with slag cement concretes

In /8/ a series of capillary absorption tests of concretes made with slag cements are presented. Four different cements made of a blend of the same clinker and the same ground granulated blast furnace slag was tested. The slag content was 0 %, 15 % ,40 % and 65 %. The w/c-ratio was 0,45 in all concretes. The nominal air contents of the concretes were 2 % (non-air entrained), 4,5 % and 6 %. The real air content differed a bit from the nominal values.

The air pore structure of some of the concretes was determined by automatic image analysis. The water absorption was followed up to 30 days. One example of a water absorption test is shown in Fig 5.1. All results are presented in the original report /8/

The degree of saturation of the airpore system versus the time counted from the nick-point time was analyzed according to Eq (5.1) and (5.2). The results are listed in Table 5.1. A measure of the absorption rate is obtained by calculating the time needed for a certain fraction of the airpore system to become water-filled. For S_a=0,50 this time is $t_{0,5}$. It is calculated by Eq (5.3).

$$t_{0,5} = [0,5/A]^{1/B} \qquad (5.3)$$

All results of the calculations for the individual concretes are listed in Table 5.1. In Table 5.2 the mean values and the spread in the coefficients A and B are listed for each cement type separately but including all concretes with the same cement but with different air contents.

The spread in the results is not so large. It is a general trend that the exponent B increases with the slag content. The coefficient A is more constant. Therefore, the time for 50 % absorption in the airpore system $t_{0,5}$ decreases considerably

with increasing slag contant; see Fig 5.2 and Table 5.3. This means that the service life is very much reduced when a cement with high slag content is used. The reason might be that the pore structure becomes finer the more slag is used in the cement; see Fig 5.3 which shows the specific surface of the entire airpore system versus the slag and air contents.

The time $t_{0,5}$ is almost independent of the total air content which strengthens the theoretical analysis; viz. it implies that an airpore of a certain size is filled within about the same time irrespectively of the number of pores. This is in accordance with the theory.

The exponent B is low enough to indicate that Model 2 of the absorption process is valid. The pore size distribution is known; see Fig 5.4. Therefore, a detailed calculation of the absorption process based on the principles in section 3 could be performed. This is not done in this report. Only an approximative calculation for the pure portland cement concretes is performed.

The size distribution resembles the power function. The following frequency function describes the measured distribution for pores smaller than 300μ m in a fair way; see /8/:

$$f(r) = a_2 \cdot \frac{1}{r^3} \qquad (r<300\ \mu m) \qquad (5.4)$$

The exponent 3 is of the correct order of size for airpore systems of normal size distribution and shape; see section 4.2.3.

The theoretical solution of the power function for Model 2 is given in eq (4.41). It can be compared with the mean relation for the portland cement concretes which is ; see Table 5.2:

$$S_a(t) = 6{,}36 \cdot 10^{-3} \cdot t^{0{,}245} \qquad (5.5)$$

Thus, the exponent 0,245 shall be compared with the theoretical in eq (4.41). Then, the specific surface of the entire airpore system can be calculated:

$$0{,}245 = 1{,}46 \cdot \alpha_o^{-0{,}49} \qquad (5.6)$$

$$\alpha_o = 38\ mm^{-1} \qquad (5.7)$$

This value is of the correct order of size; the average value for all the three concretes is 32 mm^{-1}; see Table 5.1.

The coefficient $6{,}36 \cdot 10^{-3}$ in eq (5.5) shall be compared with the theoretical in eq (4.41). Then, the diffusivity of dissolved air δ can be calculated:

$$6{,}36 \cdot 10^{-3} = 1{,}33 \cdot 10^{-8} \cdot 38^{3{,}58} \cdot [q'/\rho_o]^{0{,}245} \qquad (5.8)$$

Where the density of air ρ_o is $1,25 \cdot 10^{-18}$ kg/μm^3. Then, the diffusion rate q´is:

$$q' = [4,34 \cdot 10^{-5}]^{1/0,245} = 1,56 \cdot 10^{-18} \quad [kg/s] \qquad (5.9)$$

But q´is obtained by eq (3.33).

$$q' = \delta \cdot [1+1/5] \cdot 4\pi \cdot 2,5 \cdot 10^{-7} \cdot 2 \cdot 0,074 = 5,6 \cdot 10^{-7} \cdot \delta \qquad (5.10)$$

Where δ is the diffusivity searched for. Insertion of eq (5.10) in (5.9) gives:

$$\mathbf{d = 2,8 \cdot 10^{-12} \quad [m^2/s]} \qquad (5.11)$$

Thus, both the calculated value of the specific surface ao and the diffusivity are of the right order of size.

Table 5.1: Results of capillary absorption tests of slag cement concretes. The total test time is 30 days.

slag cont. (%)	air cont. (%)	α_o mm^{-1}	S_n	A in Eq(5.2)	B in Eq(5.2)	$t_{0,5}$ (sec.)
	2,1	16	0,855	$6,55 \cdot 10^{-3}$	0,253	$2,8 \cdot 10^7$
0	4,5	36	0,713	$6,22 \cdot 10^{-3}$	0,238	$1,0 \cdot 10^8$
	6,2	45	0,639	$6,31 \cdot 10^{-3}$	0,244	$6,1 \cdot 10^7$
	2,0	23	0,859	$9,94 \cdot 10^{-3}$	0,238	$1,4 \cdot 10^7$
15	4,1	54	0,729	$7,16 \cdot 10^{-3}$	0,247	$2,9 \cdot 10^7$
	5,9	44	0,633	$7,47 \cdot 10^{-3}$	0,248	$2,3 \cdot 10^7$
	2,2	52	0,878	$6,24 \cdot 10^{-3}$	0,277	$7,5 \cdot 10^6$
	4,2	40	0,765	$5,85 \cdot 10^{-3}$	0,268	$1,6 \cdot 10^7$
40	5,4	55	0,693	$4,71 \cdot 10^{-3}$	0,286	$1,2 \cdot 10^7$
	4,2	52	0,750	$5,59 \cdot 10^{-3}$	0,274	$1,3 \cdot 10^7$
	6,8		0,652	$6,32 \cdot 10^{-3}$	0,272	$9,5 \cdot 10^6$
	1,8	26	0,879	$6,28 \cdot 10^{-3}$	0,281	$5,8 \cdot 10^6$
65	3,3	43	0,825	$6,85 \cdot 10^{-3}$	0,277	$5,3 \cdot 10^6$
	4,5	50	0,775	$7,55 \cdot 10^{-3}$	0,268	$6,2 \cdot 10^6$
	6,0	49	0,688	$5,50 \cdot 10^{-3}$	0,289	$6,0 \cdot 10^6$
Average values		32		$6,67 \cdot 10^{-3}$	0,264	$1,3 \cdot 10^{7}$ 1)

1) Based on the average values of all values of A and B.

Table 5.2: The mean values of the coefficients A and B and the standard deviations in these values for the different cement types.

Slag content (%)	A		B	
	mean	stand. dev	mean	stand dev.
0	$6,36 \cdot 10^{-3}$	$0,17 \cdot 10^{-3}$	0,245	0,08
15	8,19·	1,52·	0,244	0,06
40	5,74·	0,65·	0,275	0,07
65	6,55·	0,87	0,279	0,11

Table 5.3: The time needed to water-fill 30, 50 and 70 % of the airpore system. The calculation is based on the mean coefficients of A and B from Table 5.2.

Slag content (%)	time (days)		
	$t_{0,3}$	$t_{0,5}$	$t_{0,7}$
0	80	640	2550
15	30	240	960
40	20	130	450
65	10	70	220

5.3 Tests of cement mortars

The long term water absorption has been determined for nine different cement mortars exposed to more than 250 days of uninterrupted water suction /9/. The cement was of type OPC. Three different w/c-ratios were tested. For every w/c-ratio three different air contents were investigated. The airpore characteristics are unknown. The cement mortars were rather old when the test started; three pre-curing times were used; (i) 70 to 150 days, (ii) 170 to 240 days, (iii) 240 to 290 days.

The results are evaluated by Eq (5.1) and (5.2). The results are listed in Table 5.4.

Generally, the coefficient A is smaller than for the slag cement concretes and the exponent B is larger, the net effect being that the time $t_{0,5}$ needed to fill 50 % of the airpore system is somewhat shorter than was found for the pure portland cement concretes in section 5.2.

The big spread in the results is probably to a large extent depending on the fact that the airpore structure is different in different specimens. In a specimen containing a large amount of fine pores the absorption rate is much more rapid than in a more coarse-porous specimen.

It is must also be observed that it is rather difficult to measure the weigh gain of a specimen with a sufficiently high precision after a long time of absorption when the water absorption is very slow.

Example: Consider a specimen of the actual size 50·120·20 mm made of a cement mortar with the w/c-ratio 0,55, the cement content 500 kg/m^3 and the air content 9 %. The total pore volume in such a specimen is about 35 cm^3. The air volume is 11 cm^3. The total weight of a saturated specimen is about 290 g.

The weight gain during 1 month of absorption when 200 days of water uptake has already occured is estimated by the average coefficients A and B in Table 5.4. The degree of saturation of the airpore system increases from 0,458 to 0,479. This corresponds to a weight gain of only 0,23 grammes. This is very difficult to measure with a sufficiently high precision by an ordinary balance capable of measuring 300 grammes of total wight. Besides, a very small evaporation from the top surface of the specimen causes a large error in the extrapolated water absorption curve.

It is, therefore, clear that new and more precise measurement methods must be developped if the very slow absorption after a long suction time shall be monitored with a sufficiently high precision. An imaginable method is to keep the specimen immersed in water during the whole test and weigh the specimens when still immersed.

Table 5.4: Results of long term capillary absorption tests of cement mortars. The test time is 200 to 250 days.

w/c (air) (%)	age	S_n	A in Eq(5.2)	B in Eq(5.2)	r^2 1)	$t_{0,5}$ (sec)
0,40	114	0,826	$8,91 \cdot 10^{-5}$	0,500	0,95	$3,1 \cdot 10^{7}$
	226	0,867	$2,35 \cdot 10^{-3}$	0,325	1,00	$1,5 \cdot 10^{7}$
(4,3)	288	0,878	$2,45 \cdot 10^{-3}$	0,324	0,99	$1.3 \cdot 10^{7}$
0,40	107	0,741	$1,17 \cdot 10^{-4}$	0,437	0,96	$2,0 \cdot 10^{8}$
	219	0,784	$1,39 \cdot 10^{-3}$	0,327	0,98	$6,6 \cdot 10^{7}$
(7,0)	275	0,815	$3,51 \cdot 10^{-4}$	0,261	0,95	$1,2 \cdot 10^{12}$
0,40	120	0,702	$1,93 \cdot 10^{-3}$	0,310	0,99	$6,1 \cdot 10^{7}$
	204	0,713	$2,06 \cdot 10^{-3}$	0,313	0,99	$4.2 \cdot 10^{7}$
(8,2)	260	0,710	$1,83 \cdot 10^{-3}$	0,334	0,99	$2,0 \cdot 10^{7}$
0,55	147	0,749	$5,98 \cdot 10^{-3}$	0,199	0,88	$4,6 \cdot 10^{9}$
	231	0,785	$1,55 \cdot 10^{-3}$	0,316	0,97	$8,7 \cdot 10^{7}$
(6,6)	287	0,754	$1,87 \cdot 10^{-3}$	0,336	0,98	$1,7 \cdot 10^{7}$
0,55	113 2)	0,663	$5,88 \cdot 10^{-3}$	0,185	0,88	$2,7 \cdot 10^{10}$
	197	0,650	$1,13 \cdot 10^{-3}$	0,313	0,96	$2,8 \cdot 10^{8}$
(9,5)	253	0,637	$5,98 \cdot 10^{-4}$	0,394	0,96	$2,6 \cdot 10^{7}$
0,55	107 2)	0,505	$3,25 \cdot 10^{-3}$	0,202	0,91	$6,7 \cdot 10^{10}$
	191	0,519	$2,18 \cdot 10^{-4}$	0,409	0,96	$1,7 \cdot 10^{8}$
(14,3)	247	0,526	$6,24 \cdot 10^{-4}$	0,390	0,97	$2,8 \cdot 10^{7}$
0,70	153 2)	0,761	$2,19 \cdot 10^{-3}$	0,287	1,00	$1,7 \cdot 10^{8}$
	237	0,770	$4,65 \cdot 10^{-4}$	0,400	0,91	$3,8 \cdot 10^{7}$
(8,0)	293	0,776	$2,51 \cdot 10^{-3}$	0,310	0,97	$2,6 \cdot 10^{7}$
0,70	85 2)	0,690	$4,77 \cdot 10^{-3}$	0,185	0,94	$8,3 \cdot 10^{10}$
	169	0,725	$9,53 \cdot 10^{-3}$	0,186	0,91	$1,8 \cdot 10^{9}$
(9,2)	225	0,643	$3,11 \cdot 10^{-3}$	0,298	1,00	$2,5 \cdot 10^{7}$
0,70	70	0,544	$4,06 \cdot 10^{-5}$	0,514	0,95	$9,1 \cdot 10^{7}$
	182	0,564	$1,13 \cdot 10^{-4}$	0,452	0,93	$1,2 \cdot 10^{8}$
(14,2)	238	0,520	$2,54 \cdot 10^{-3}$	0,302	1,00	$4,0 \cdot 10^{7}$
Average values			$2,18 \cdot 10^{-3}$	0,326		$1,7 \cdot 10^{7}$

1) Correlation coefficient
2) The result is unreliable since a certain drying has occured during a period of the test

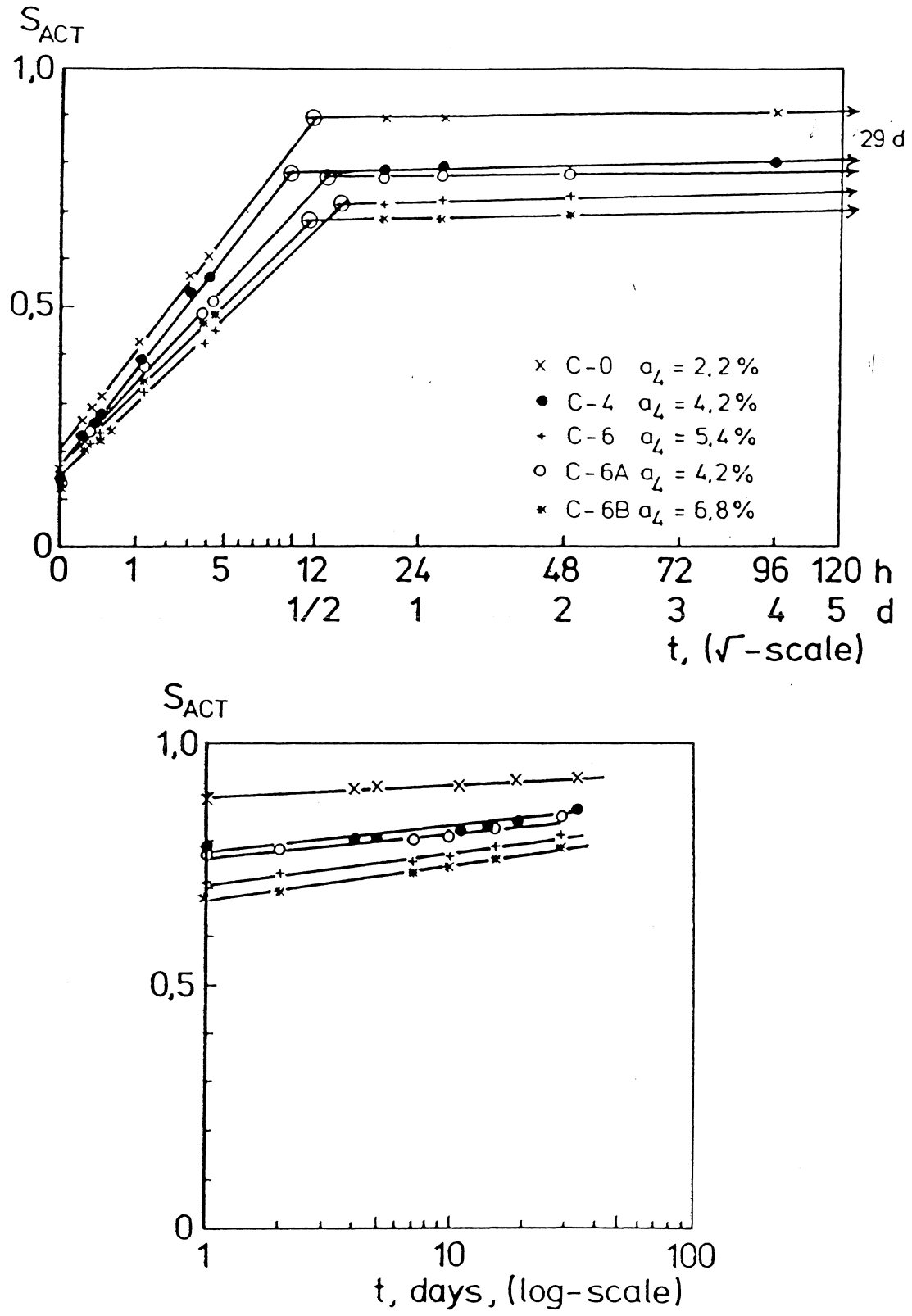

Fig 5.1: Example of the result of water uptake tests of slag cement concretes; /8/. Slag content 40 %, w/c-ratio 0,45, 5 different air contents (a_4 is the air content of the fresh, poker-vibrated concrete).

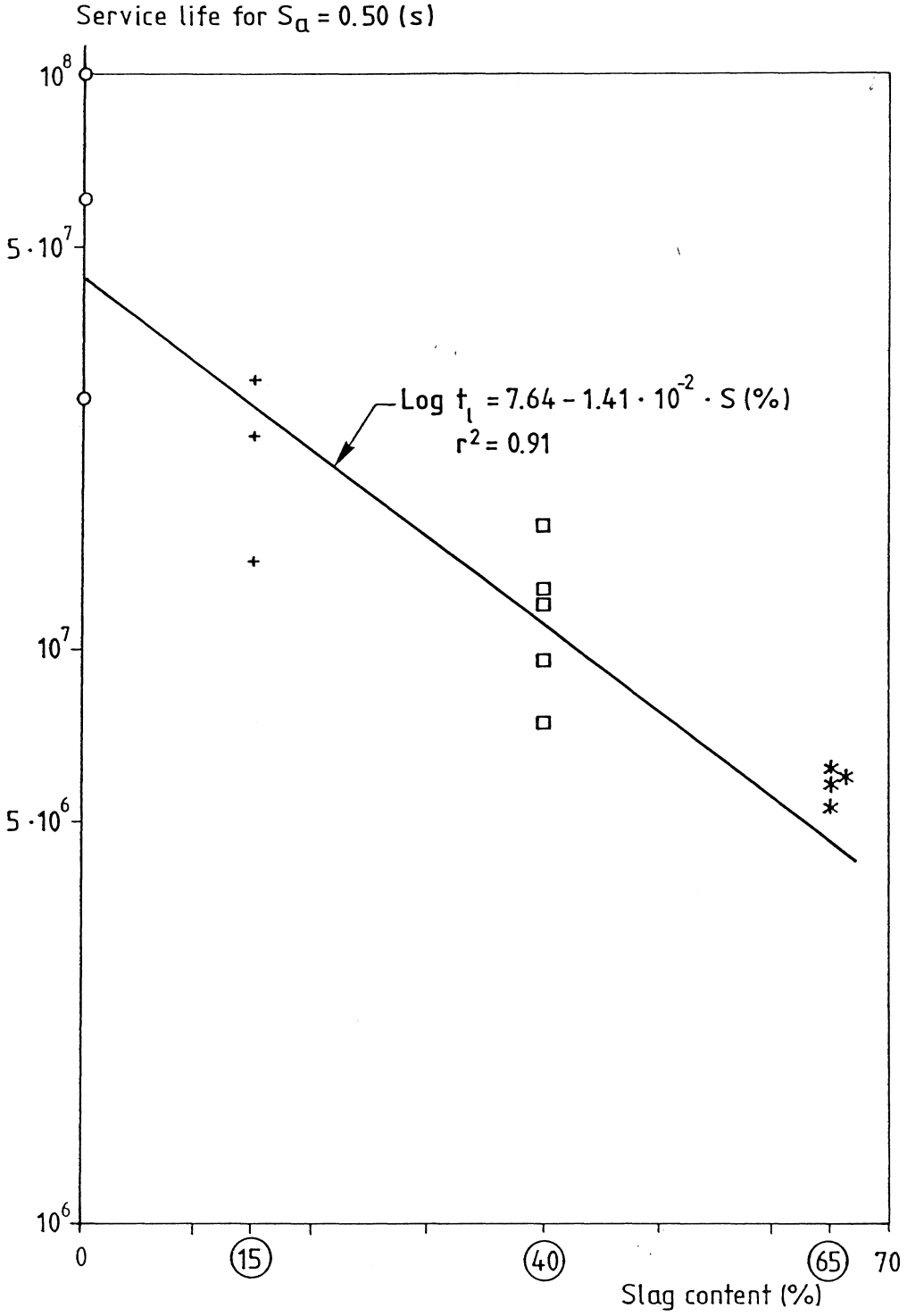

Fig 5.2: The time $t_{0,5}$ needed to fill 50 % of the airpore system, versus the slag content of the cement. Constant w/c-ratio 0,45. Different air contents. Data from Table 5.1.

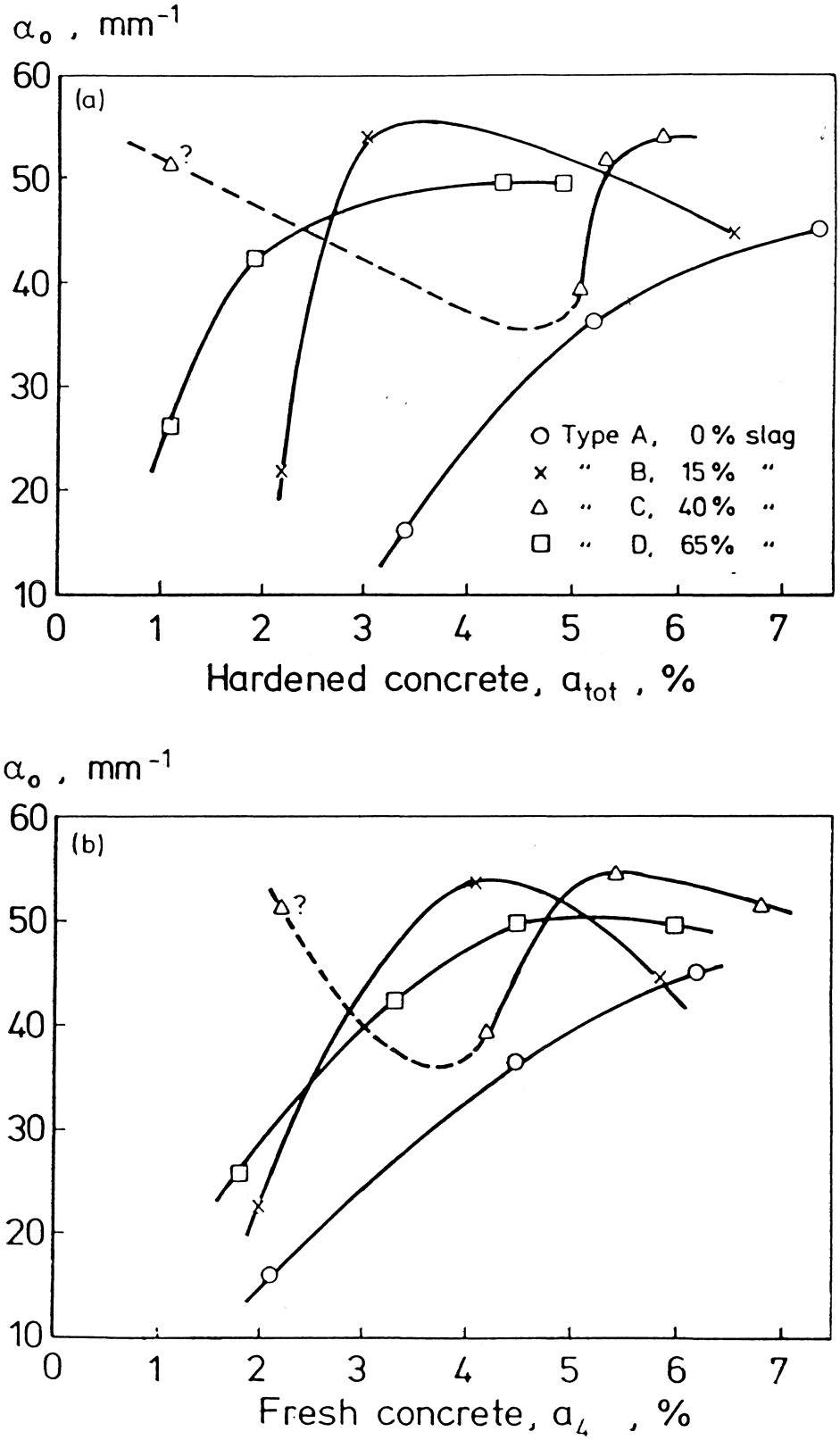

Fig 5.3: Relation between the air content of the hardened or fresh concrete and the specific surface α_o of the entire airpore system. The same concretes as in Table 5.1.

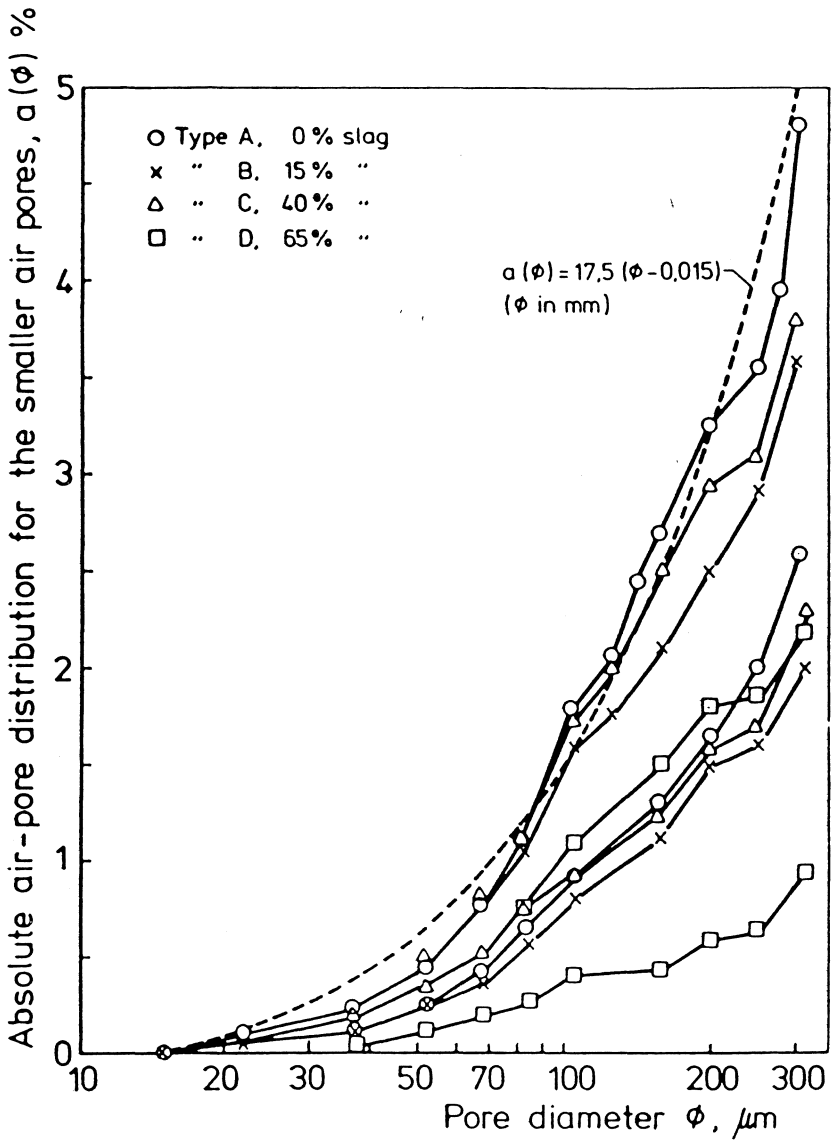

Fig 5.4: The airpore distribution of the concretes i Table 5.1.

Summary

Frost damage occurs when a certain critical water content in the pore system of the concrete is transgressed. Below the critical water content no harm is caused when the concrete freezes; above the critical value severe damage occurs. Therefore, the residual service life of concrete that is exposed to frost action is coupled to the future moisture conditions inside the concrete. The critical absorption is individual for each concrete and depends on its water-cement ratio, its air content, its airpore structure etc. It is almost independent of the number of freeze/thaw cycles and the freezing rate but it is to a certain extent dependent of the minimum freezing temperature.

The critical water content is a "fracture value" that is individual for every concrete. It does always correspond to a certain absorption in the so called airpores by which is meant pores that are coarse enough not to take part in the capillary absorption process. Therefore, in order to make a prediction of the future service life possible one has to be able to predict the long term absorption in the airpore system.

In this report a theoretical and quantitative analysis is made of the absorption process in airpores within a concrete that is permanently stored in water. The absorption depends on the dissolution of air from airbubbles that became enclosed in the airpores already during the first rapid capillary absorption process. The dissolved air moves by diffusion to larger airbubbles and, finally, to the surface of the specimen. This process is very slow, especially for coarse airbubbles .

Two models for the absorption process are treated;

Model 1: According to which water absorption takes place simultanously in bubbles of all sizes. It leads to a rather rapid water absorption process, the smallest bubbles being lost at first but the coarser bubbles also absorbing water from the onset of water storage.

Model 2: According to which a coarser bubble does not start to absorb water until the next smaller bubble is completely filled. This model is the most plausible one from a thermodynamical point of view. It leads to a considerably slower absorption rate than Model 1 and, thus, to a longer service life.

Equations for calculation of the water absorption in an arbritary airpore system are provided. Two types of frequency curves of the pore radius are investigated in detail; (i) exponential functions; (b) power functions. Diagrams for the prediction of the absorption-time curves in such pore systems are provided.

The absorption rate is found to be very much depending on the shape of the pore size distribution; the exponential function giving much more rapid absorption at a given average specific surface of the airpore system.

Experimental long term water absorptions for 15 concretes and 27 cement mortars are presented. The agreement between the theoretical absorption curves and the observed is fairly good. It seems as if Model 2 is in better agreement with the measurements than is Model 1.

References

/1/ Fagerlund G: The critical size in connection with freezing of porous materials. Cementa Report CMT 86039, Stockholm 1986.

/2/ Fagerlund G: Influence of slag cement on the frost resistance of concrete - a theoretical analysis. Swedish Cement and Concrete Research Institute. Research Fo 1:80, Stockholm, 1980.

/3/ Fagerlund G: Effect of the freezing rate on the frost resistance of concrete. Nordic Concrete Research, Publication Nr 11, Oslo 1992.

/4/ Powers T.C: The air requirement of frost resistant concrete. Proceedings Highway Research Board, Vol 29, 1949.

/5/ Fagerlund G: Equations for calculating the mean free distance between aggregate particles or airpores in concrete. Swedish Cement and Concrete Research Institute. Research Fo 8:77, Stockholm 1977.

/6/ Fagerlund G: The critical degree of saturation method of assessing the freeze/thaw resistance of concrete. Materials and Structures, Vol 10, No 58, 1977.

/7/ Fagerlund G: Prediction of the service life of concrete exposed o frost action. Article in "Studies on Concrete Technology". Swedish Cement and Concrete Research Institute. Stockholm 1979.

/8/ Fagerlund G: The influence of slag cement on the frost resistance of the hardened concrete. Swedish Cement and Concrete Research Institute. Research Fo 1:82, Stockholm 1982.

/9/ Rombén L: Unpublished test results of the long term water absorption in cement mortars. Swedish Cement and Concrete Research Institute, 1974.

APPENDIX 1: Model 1. Calculated real degree of saturation of the airpore system. Exponential function.

i	$r_{m,i}$	$t \cdot q' / \rho_o$ or $\frac{4\pi}{3} \cdot (r_{m,1})^3$	S_a the specific surface α_o mm^{-1}				
	(μm)		50	40	30	20	10
1	15	$1,4 \cdot 10^4$	0,041	0,024	0,011		
1´	20	3,3				0,008	0,001
2	25	6,5	0,133	0,083	0,042		
3	35	$1,8 \cdot 10^5$	0,259	0,172	0,094		
3´	40	2,7				0,049	0,008
4	45	3,8	0,391	0,274	0,161		
5	55	7,0	0,519	0,382	0,240		
5´	60	9,0				0,122	0,024
6	65	$1,2 \cdot 10^6$	0,636	0,501	0,331		
7	75	1,8	0,734	0,591	0,411		
7´	80	2,1				0,218	0,047
8	85	2,6	0,803	0,671	0,490		
9	95	3,6	0,857	0,738	0,561		
9´	100	4,2				0,328	0,080
10	105	4,9	0,901	0,800	0,628		
11	115	6,4	0,930	0,844	0,687		
11´	120	7,2				0,431	0,120
12	125	8,2	0,950	0,880	0,737		
13	135	$1,0 \cdot 10^7$	0,964	0,901	0,785		
13´	140	1,1				0,525	0,160
14	145	1,3	0,974	0,929	0,820		
14´	160	1,7				0,653	0,213
15	175	2,2	0,995	0,978	0,914		
15´	180	2,4				0,691	0,265
15´´	200	3,3				0,756	0,317
15´´´	220	4,5				0,816	
16	225	4,8	0,997	0,991	0,975		
16´	235	5,4					0,420
16´´	240	5,8				0,856	
17	275	8,7	1,000	1,000	0,993	0,919	
17´	285	9,7					0,548
18	325	$1,4 \cdot 10^8$			0,999	0,959	
18´	335	1,6					0,655
19	375	2,2			1,000	0,981	
19´	385	2,4					0,747
20	425	3,2				0,991	
21	435	3,4					0,808
22	485	4,8					0,864
23	535	6,4					0,902
24	585	8,4					0,934
25	685	$1,3 \cdot 10^9$				1,000	0,968
26	860	2,7					0,993

APPENDIX 2: Model 1. Calculated effective degrees of saturation of the airpore system. Exponential function.

i	$r_{m,i}$	$t \cdot q'/\rho o$ or $\frac{4\pi}{3} \cdot (r_{m,i})^3$	$S_{a,eff}$ the specific surface α_o mm^{-1}				
	(μm)		50	40	30	20	10
1	15	1,4·104	0,016	0,008	0,003		
1´	20	3,3				0,003	0,0002
2	25	6,5	0,062	0,033	0,014		
3	35	1,8·105	0,140	0,079	0,034		
3´	40	2,7				0,018	0,002
4	45	3,8	0,238	0,144	0,067		
5	55	7,0	0,346	0,224	0,113		
5´	60	9,0				0,052	0,005
6	65	1,2·106	0,463	0,314	0,170		
7	75	1,8	0,571	0,407	0,234		
7´	80	2,1				0,105	0,013
8	85	2,6	0,664	0,495	0,303		
9	95	3,6	0,742	0,577	0,373		
9´	100	4,2				0,177	0,025
10	105	4,9	0,806	0,652	0,440		
11	115	6,4	0,854	0,717	0,507		
11´	120	7,2				0,262	0,042
12	125	8,2	0,894	0,771	0,570		
13	135	1,0·107	0,923	0,817	0,626		
13´	140	1,1				0,349	0,064
14	145	1,3	0,946	0,859	0,679		
14´	160	1,7				0,440	0,090
15	175	2,2	0,991	0,962	0,862		
15´	180	2,4				0,521	0,121
15´´	200	3,3				0,599	0,157
15´´´	220	4,5				0,671	
16	225	4,8	0,998	0,993	0,951		
15´	235	5,4					0,224
16´´	240	5,8				0,733	
17	275	8,7	1,000	1,000	0,985	0,849	
17´	285	9,7					0,370
18	325	1,4·108			0,946	0,918	
18´	335	1,6					0,485
19	375	2,2			1,000	0,958	
19´	385	2,4					0,587
20	425	3,2				0,980	
21	435	3,4					0,674
22	485	4,8					0,749
23	535	6,4				0,985	0,809
24	585	8,4					0,860
25	685	1,3·109				1,000	0,923
26	860						0,984

APPENDIX 3: Calculated real and effective degrees of saturation of the airpore system. Power function.

1	$r_{m,i}$ (μm)	$t \cdot q'/\rho_o$ or $\frac{4\pi}{3} \cdot (r_{m,i})^3$	The specific surface α_o (mm^{-1}) 50		30		10	
			S_a	$S_{a.eff}$	S_a	$S_{a,eff}$	S_a	$S_{a,eff}$
1	20	$3,3 \cdot 10^4$	0,090	0,068	0,034	0,025	0,003	0,002
2	40	$1,7 \cdot 10^5$	0,174	0,156	0,079	0,069	0,021	0,007
3	60	9	0,259	0,217	0,129	0,104	0,022	0,014
4	80	$2,1 \cdot 10^6$	0,316	0,267	0,170	0,136	0,038	0,022
5	100	4,2	0,365	0,309	0,210	0,166	0,054	0,031
6	120	7,2	0,406	0,345	0,249	0,194	0,075	0,041
7	140	$1,1 \cdot 10^7$	0,440	0,378	0,281	0,221	0,089	0,051
8	160	1,7	0,476	0,409	0,316	0,248	0,111	0,063
9	180	2,4	0,505	0,437	0,345	0,272	0,130	0,075
10	200	3,3	0,526	0,462	0,373	0,297	0,151	0,089
11	250	6,5	0,606	0,521	0,449	0,354	0,212	0,124
12	300	$1,1 \cdot 10^8$	0,652	0,570	0,509	0,408	0,272	0,163
13	350	1,8	0,704	0,616	0,573	0,458	0,341	0,207
14	400	2,7	0,748	0,657	0,632	0,506	0,410	0,252
15	450	3,8	0,785	0,696	0,679	0,554	0,474	0,301
16	500	5,2	0,816	0,731	0,723	0,601	0,535	0,352
17	600	9,0	0,880	0,796	0,815	0,688	0,670	0,465
18	700	$1,4 \cdot 10^9$	0,927	0,854	0,994	0,770	0,784	0,584
19	800	2,1	0,963	0,906	0,941	0,851	0,886	0,715
20	900	3,0	0,987	0,955	0,978	0,926	0,956	0,852
21	1000	4,2	1,000	1,000	1,000	1,000	1,000	1,000

APPENDIX 4: Properties of air

1. Density of air.

The density of air can be calculated by; /A1/.

$$\gamma_a = 1{,}293 \cdot \frac{273{,}15}{T} \cdot \{\frac{B - 0{,}3783 \cdot e}{760}\} \qquad (A.1)$$

Where B is the air-pressure and e is the water vapour pressure, both in mm Hg. T is the absolute temperature.

The following data are valid for dry air or air at RH 100%, in both cases at 760 mm air pressure.

Table A.1: Density of dry or moist air at 760 mm Hg.

Temperature (°C)	e (mm Hg)	Density, γ_a Dry air	RH 100%
0	4,9	1,293	1,290
+5	6,8	1,270	1,266
+10	9,4	1,247	1,242
+15	12,8	1,226	1,218
+20	17,3	1,205	1,194
+25	23,0	1,185	1,171
+30	30,4	1,165	1,147

2. Solubility of air in water

The solubility of air in water is x (mol air)/(mol water) or $x/18 \cdot 10^{-6}$ (mol air)/(m^3 water).

The corresponding air volume, V_a, at the actual temperature T is:

$$V_a = \frac{x}{18 \cdot 10^{-6}} \cdot \frac{RT}{P} \quad [m^3 \text{ air}/m^3 \text{ water}] \qquad (A.2)$$

Where R is the general gas constant (8,314 J/K·mol) and P is the pressure. For $P=10^5$ Pa (1 atm), eq (A.2) is written:

$$V_a = 4{,}619 \cdot T \cdot x \quad [m^3 \text{ air}/m^3 \text{ water}] \qquad (A.3)$$

The weight of dissolved air is:

$$Q_a = V_a \cdot \gamma_a \quad [kg/m^3] \qquad (A.4)$$

Where γ_a is the density of air. With inserted coefficients at 1 atm pressure:

$$Q_a = 4,619 \cdot T \cdot \gamma_a \cdot x \quad [kg/m^3] \qquad (A.5)$$

The solubility x is given in handbooks, e,g, /A.1/. The air density is given in Table A.1.

Calculated values of V_a and Q_a are listed in Table A.2.

Table A.2: The solubility of air in water.

Temperature (°C)	Solubility x (mol/mol)	Volume of dissolved air (m^3/m^3)	Weight of dissolved air (kg/m^3)
0	$2,316 \cdot 10^{-5}$	0,0292	0,0377
+5	2,042·	0,0262	0,0332
+10	1,824·	0,0239	0,0297
+15	1,647·	0,0219	0,0267
+20	1,504·	0,0204	0,0244
+25	1,388·	0,0191	0,0224
+30	1,293·	0,0181	0,0208

A.3. Diffusivity of air in water

At +25 °C the diffusivity of air in water, $\delta_{a,w}$, is $2 \cdot 10^{-9}$ m^2/s; see /A.1/.

The diffusivity at other temperatures is supposed to be approximately proportional to the absolute temperature; /A.2/:

$$\delta_{a,w} = 2 \cdot 10^{-9} \cdot \frac{T}{298} \qquad (A.6)$$

Literature:

/A.1/ Handbook of Chemistry and Physics.

/A.2/ Bird R.B., Stewart W.E, Lightfoot E.N: Transport phenomena. John Wiley & Sons, Inc. New York, London, Sidney, 1960.